Supplement of Atmos. Chem. Phys., 20, 9997–10014, 2020
https://doi.org/10.5194/acp-20-9997-2020-supplement

Atmospheric Chemistry and Physics
Open Access
EGU

Supplement of

Polycyclic aromatic hydrocarbons (PAHs) and oxy- and nitro-PAHs in ambient air of the Arctic town Longyearbyen, Svalbard

Tatiana Drotikova et al.

Correspondence to: Tatiana Drotikova (tatiana.drotikova@unis.no)

Table of Contents

Text S1. Analytical procedures

Chemicals

Dichloromethane (DCM), *n*-hexane, and acetone (GC–MS grade), were purchased from VWR International AS, Oslo, Norway. Standards of PAHs, nitro- and oxy-PAHs in *c*-hexane (>98.0 % purity) were purchased from Chiron AS, Trondheim, Norway.

Sample preparation

QFFs (particulate phase) and PUFs (gaseous phase) samples were extracted separately by two different methods, followed by the same clean-up procedure. Fifty ng of 25 ^{2}H-labelled PAH (dPAH) internal standards (ISTDs), including 16 EPA priority dPAHs (Table S4), 3 dOxy-PAHs, and 6 dNitro-PAHs (Table S5), were added before extraction. Previously reported methods (Albinet et al., 2006; Albinet et al., 2013; Albinet et al., 2014) were combined, modified and validated for the current trace quantitative analysis. QFF was placed in a centrifuge glass tube. After addition of 12-15 mL DCM, the tube was vortexed for 1.5 min (VWR 12620-848, Oslo, Norway). The sample was then centrifuged (Hettich, Universal 320, Germany) for 5 min at 4,000 rpm at 10°C and the supernatant was transferred to a clean glass vial. The extraction procedure was repeated three times. Combined supernatants (about 40 ml) were concentrated to about 500 µL under gentle nitrogen stream (5.5 quality; AGA, Norway) using Reacti-vap 18780 (Pierce Biotechnology Inc., Sweden). PUF samples were Soxhlet extracted with DCM for 24 hours. The extract (about 300 mL) was reduced to about 500 µL (Zymark, Turbovap 500, Sweden).

The QFF and PUF extracts were first cleaned on neutral alumina Al_2O_3 SPE cartridge (500 mg, Macherey Nagel, Germany). PAHs, nitro- and oxy-PAHs were eluted with 9 mL DCM. After concentration under a gentle nitrogen stream, the residue was dissolved in 200 µL *n*-hexane. Samples were further cleaned-up with neutral silica SiO_2 SPE cartridge (500 mg, Macherey Nagel, Germany). The alkane fraction was eluted with 1 mL *n*-hexane and discarded. PAHs, nitro- and oxy-PAHs were thereafter eluted with 9 mL 35:65 (v/v) DCM-*n*-hexane. The elute was dried under a gentle nitrogen stream and redissolved in 100 µL *n*-hexane. Subsequently, the purified samples were spiked with 10 ng of three recovery standards (RSTDs; 1,2,3,4-tetrachloronaphthalene, Flt-d10, and 1-NPyr-d9) and analyzed by GC-MS.

GC-MS analysis

16 priority PAHs, 8 oxy-PAHs, and 21 nitro-PAHs were analyzed via two different methods using a 7890B Agilent GC chromatograph coupled to 7000C Agilent Triple Quad MS (Agilent Technologies, Santa Clara, California). All compounds were separated on the low-polar TG-5SILMS capillary column (5% Phenyl Methylpolysiloxane; 30 m with 5 m safe guard × 0.25 mm × 0.25 μm film thickness; cat. 26096-1425, Thermo Scientific Trace GC Ultra. A sample injection volume was 1 μL; pulsed splitless injection mode using a 4 mm ID splitless, single taper, no wool ultra inert liner (5190-2292, Agilent, USA). Agilent MassHunter software (Version B.07.00 /Build 7.0.457.0, 2008) was used for instrument control, method validation and quantification.

PAH analysis by GC–EI-MS/MS method

The injector temperature was 300 °C in pulsed splitless mode at 35 psi for 1.5 min (1.6 min splitless time). Ultra pure He (quality 6.0; AGA, Norway) was used as carrier gas, at a constant flow rate of 1.0 mL min-1. The GC oven temperature program was as follows: initial temperature was hold at 70 °C for 3 min, increased to 170 °C at 40 °C min-1, with further increase to 240 °C at 10 °C min-1, followed by a ramp to 310 °C at 5 °C min-1 and hold for 2 min. Transfer line temperature was 325 °C. The ion source temperature was 280 °C and quadrupoles temperatures were 150 °C.

The MS was run in electron ionization (EI) mode. The solvent delay time was 5.0 min. Nitrogen (quality 6.0; AGA, Norway) was used as collision gas at a flow rate of 1.5 mL min-1. Helium quench gas was set at 2.25 mL min-1. Electron ionization was operated at 70 eV. Analyses were performed in multiple reaction monitoring (MRM) mode. Table S4 gives the retention times (RTs) and the monitored transitions for each compound and collision energy adopted from (Kanan et al., 2012). For the deuterated internal standards, the chosen transitions were parent molecular ion-parent molecular ion, at collision energy 0 eV.

Nitro- and oxy-PAH analysis by GC-ECNI-MS method

The injector temperature was 230 °C in pulsed splitless mode at 40 psi for 1.5 min (1.6 min splitless time). The carrier gas (He) flow rate was 1.2 mL min^{-1}. The GC temperature program started at 70 °C for 2 min, then ramped to 250 °C at 45 °C min^{-1} and held for 5 min, followed by a ramp to 310 °C at 5 °C min^{-1}. Transfer line temperature was 325 °C.

The MS was run in electron capture negative ion (ECNI) mode. The MS parameters were as follows: ion source temperature was 280 °C and quadrupole temperature was 150 °C. Methane (quality 6.0; AGA, Norway) was used as a reagent gas with a flow of 2.5 mL min^{-1}, electron energy was 150 eV and the emission current was 50 μA. Analyses were performed in selected ion monitoring mode (SIM). Monitored ions and RT are shown in Table S5.

Text S2. Method validation and quality control

Calibration

Quantification of each individual PAH was based on eight-point calibration curve from 1 to 600 pg μL^{-1} (gravimetrically diluted) in *n*-hexane. Calibration curves were linear with $R^2 > 0.987$ for all compounds. Quantification of nitro- and oxy-PAHs was based on nine-point calibration curves from 0.5 to 400 pg μL^{-1} (gravimetrically diluted) in *n*-hexane. Calibration curves were linear with $R^2 > 0.99$ for all compounds. The linear range of 9,10-PheQ was from 5 pg μL^{-1} to 400 pg μL^{-1} with R^2 of 0.97. Individual calibration curves for all

ISTDs were based on eight concentration levels (5-250 pg μL^{-1}) with constant concentration of RSTDs (100 pg μL^{-1}), prepared in *n*-hexane.

Recovery rates

Apparent recovery (Recovery, %) for all analytes was calculated using Eq. (1):

$$\text{Recovery}, \% = \frac{M_{exp}}{M_{ref}} \times 100, \quad (1)$$

where M_{exp} is amount of target compound experimentally obtained from calibration graph and M_{ref} is a known added amount (Burns et al., 2002). Recovery of ISTD was calculated relative to RSTD added prior to GC analysis. Recoveries of target analytes were calculated relative to ISTD for spiked samples. The spiked samples were prepared by adding a known amount of native (16 PAHs, 19 nitro-PAHs, 8 oxy-PAHs) and internal (16 dPAHs, 6 dNitro-PAHs, 2 dOxy-PAHs) standards to the blank sample material before extraction. The spiked samples were treated as real samples. Four replicate samples for each sampling material were performed (QFF, n=4 and PUF, n=4).

Detection limits

Instrumental limits of detection (LOD) and quantification (LOQ) were calculated according to the calibration curve method (Konieczka and Namieśnik, 2009; Shrivastava and Gupta, 2011; Şengül, 2016) based on residual standard deviation ($STDEV_{res}$) of the calibration curve in lowest concentration range (from 1 to 5 pg μL^{-1} for PAHs and from 0.1 to 5 pg μL^{-1} for nitro- and oxy-PAHs; n=15 measurements). $STDEV_{res}$, LOD, and LOQ were calculated by Eq. (2), (3) and (4), respectively.

$$\text{STDEVres} = \sqrt{\frac{\sum(Y-Yeq)^2}{n-2}}, \quad (2)$$

where Y is the observed value of a compound peak area and Y_{eq} is the value calculated using the determined linear regression equation.

$$LOD = 3.3 \text{ x } STDEV_{res}/\text{slope} \quad (3)$$

$$LOQ = 10 \text{ x } STDEV_{res}/\text{slope} \quad (4)$$

Samples showed analyte concentrations below limit of quantification (LOQ) were replaced by LOQ/2 for statistical analysis.

In order to evaluate the background contamination related to sample collection and analysis, PUF and QFF field blanks (exposed filters without any air filtration; n=4 for PP and n=4 for UNIS/Adventdalen) and laboratory blanks (n=3 for PP and n=3 for UNIS/Adventdalen) were treated and analyzed by the same methods as real samples. Laboratory blanks were prepared for each extraction batch. MDL was calculated based on blanks according to Eq. (5):

$$MDL = \overline{X} + 3 \times STD_b, \quad (5)$$

where $\overline{X}$ is the blank mean concentration, and STD_b is the standard deviation of the replicate blank sample concentrations.

Results of method validation and quality control

Ambient atmospheric concentrations of nitro- and oxy-PAHs are in the range of few pg m^{-3} to a few ng m^{-3}, which are about 1–3 orders of magnitude lower than those of PAHs. Thus, a sensitive GC-ECNI-MS method was applied for the trace quantification of nitro- and oxy-PAHs. PAHs were identified based on compound specific RTs and two characteristic MRM transitions, while nitro- and oxy-PAHs were identified based on their RTs and monitored ions in SIM mode. The calculated instrumental LOD and LOQ values are summarized in Table S4 and Table S5. LOQ for PAHs (GC-EI-MS/MS) ranged from 0.98 to 3.69 pg. The HMW PAHs exhibited higher LODs. This may be due to interference from the stationary phase for later-eluting compounds. LOQ for nitro-PAHs (GC- ECNI-MS) ranged from 0.09 to 2.04 pg, while LOQ for oxy-PAHs (GC- ECNI-MS) were slightly higher, and ranged from 0.49 to 5.35 pg, and LOQ for 9,10-PheQ is 26.87 pg. This is because nitro-PAHs have higher affinity for negative ion formation, while the carbonyl group within oxy-PAHs is able to stabilize the excess negative charge associated with the capture of thermal electrons within the NICI process (Han et al., 2019). The linearity of instrumental response was evaluated over the range from 1 to 600 pg μL^{-1} for PAHs and 1 to 400 pg μL^{-1} for nitro- and oxy-PAHs. High values of regression coefficient r^2 were determined: $r^2 > 0.987$ for all PAHs and $r^2 > 0.990$ for all nitro- and oxy-PAHs, except 0.97 for 9,10-PheQ.

The recoveries percent of PAHs, nitro- and oxy-PAHs and their internal standards were calculated using *spiked* QFFs and PUFs samples. The recovery percent and accuracy (%RSTD) results are summarized in Table S7. Relative standards deviations (RSTDs) were in the range 5-15%, indicating a good repeatability. The recovery rates of native compounds from *spiked QFFs* samples were in the range 38-119 % for PAHs, 43-74 % for NPAHs, and 38-57 % for OPAHs, while recoveries of labeled internal standards were 65-111% for dPAHs, 40-77% for dNitro-PAHs, and 40-41% for dOxy-PAHs. The recovery rates of native compounds from *spiked PUFs* samples were in the range 44-121 % for PAHs, 56-104 % for nitro-PAHs, and 43-110 % for Oxy-PAHs, while recoveries of labeled internal standards were 54-101% for dPAHs, 69-104% for dNitro-PAHs, 50-74% for dOxy-PAHs. Native nitro- and oxy-PAHs, such as BPyr-6, 6-NBaPyr, 1,3-, 1,6-, and 1,8-DNPyr, showed low recovery (< 30 %) and therefore were excluded from quantification in air samples.

Samples spiking test (Table S7) showed that applying individual isotope labeled ISTD for each of 16 PAHs, resulted in higher apparent recovery rates (~80%-100% for most of the compounds) compared to nitro- and oxy-PAHs, where only 8 deuterated ISTDs were used for 31 nitro- and oxy-PAHs. Recovery rates for all ISTDs showed satisfying recoveries (40 – 111%). dPAHs showed nearly equal, high extraction rates for the both methods applied for QFF and PUF spiked samples. The relatively low but still satisfying recovery for dNap, 54% for PUF and 65% for QFF, could be attributed to higher volatility of the compound, which leads to higher losses during sample preparation. dNitro- and dOxy-PAHs extracted from QFF exhibited lower recovery compared to those Soxhlet extracted from PUFs. This either indicates co-extraction of PUF matrix or higher extraction efficiency of nitro- and oxy-PAHs by hot solvent circulation through PUF over long period of time (24 h).

The ISTD recoveries obtained for QFF and PUF air samples (Table S8) were in acceptable range, 63-105 % for dPAHs, 56-69% dOPAHs, 44-89% dNAPHs.

Field (n=8) and laboratory (n=6) blanks were analysed in order to monitor and control possible contamination during sample transport and laboratory work. Method detection limit (Table S6) was determined based on blank levels. High contamination of blank samples by 9,10-PheQ (UNIS and Adventdalen), and 2-NFlu (PP) was

found. Thus, concentrations for these compounds were excluded from the final results. No blank correction was performed for the concentration calculations.

Table S1. Sampling dates and sample volumes

		Power plant			**UNIS**			**Adventdalen**
Sample	Date	Volume, m^3	Sample	Start date*	Volume, m^3	Sample	Start date*	Volume, m^3
PP1	27.09.2018	2.7	U1	28.08.2018	349.2	A1	28.08.2018	359.5
PP2	27.09.2018	3.0	U2	30.08.2018	376.1	A2	30.08.2018	349.7
PP3	27.09.2018	1.7	U4	13.09.2018	365.6	A3	06.09.2018	451.5
PP4	02.10.2018	1.5	U5	25.09.2018	384.5	A4	13.09.2018	354.2
PP5	02.10.2018	1.3	U6	26.09.2018	355.7	A5	25.09.2018	403.8
PP6	02.10.2018	1.5	U7	27.09.2018	365.2	A7	27.09.2018	272.1

*sampling duration 23-31 hours

Table S2. Meteorological data for UNIS (samples U1-U7) and Adventdalen (samples A1-A7) sampling stations

Sample name	Solar radiation, W m^{-2}	Air temp, °C	Pressure, hPa	RH, %	Specific humidity*, kg kg^{-1}	Wind from**, degree	Precipitation, mm	Type of precipitation
U1	88.7±137.6	5.2±1.0	1011.5	74.7	0.0041	130.0	0.1	rain
U2	42.2±45.3	4.7±0.9	1000.1	78.0	0.0042	230.0	4.2	rain
U4	31.0±34.7	1.2±0.9	1003.3	79.5	0.0033	150.0	0.0	-
U5	18.3±24.4	-1.1±1.3	984.3	83.7	0.0030	220.0	2.8	snow
U6	27.9±39.0	-3.3±0.5	990.4	67.5	0.0020	260.0	0.3	snow
U7	16.9±28.7	-3.1±0.4	994.2	68.9	0.0020	260.0	0.2	snow
A1	88.7±137.6	4.9±0.9	1011.5	77.0	0.0041	120.0	0.1	rain
A2	42.2±45.3	5.0±1.0	1000.1	75.4	0.0042	260.0	4.2	rain
A3	76.4±110.7	3.1±1.0	1016.9	78.9	0.0040	270.0	0.0	-
A4	31.0±34.7	0.7±0.8	1003.3	85.4	0.0033	120.0	0.0	-
A5	18.3±24.4	-1.8±1.0	984.3	82.2	0.0030	210.0	2.8	snow
A7	16.9±28.7	-2.7±0.3	994.2	63.5	0.0020	250.0	0.2	snow

*calculated according to Launiainen and Vihma (1990)
**wind roses are presented as Figure S1

Table S3. Physico-chemical properties of target compounds

Compound	Abbrevation	CAS number	Structure[1)]	Log K_{oa}[2)]	Water solubility, (estimated)[2)] mg L^{-1}	Water solubility (experimental)[2)] mg L^{-1}	Boiling point[3)] °C	Log K_{ow}[2)]
Naphthalene	Nap	91-20-3	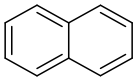	5.04	142.1	31.0	221.5±7.0	3.30
Acenaphthylene	Acy	208-96-8	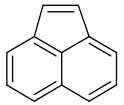	6.27	2.49	16.1	298.9±7.0	3.94
Acenaphthene	Ace	83-32-9	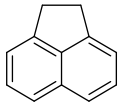	6.04	2.53	3.90	279.0±0.0	3.92
Fluorene	Flu	86-73-7	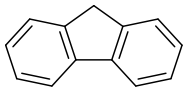	6.59	1.34	1.69	293.6±10.0	4.18
Phenanthrene	Phe	85-01-8	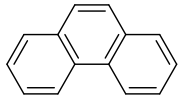	7.22	0.68	1.15	337.4±9.0	4.46
Anthracene	Ant	120-12-7	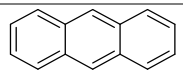	7.09	0.69	0.04	337.4±9.0	4.45
Fluoranthene	Flt	206-44-0	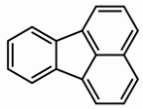	8.60	0.13	0.26	375.0±0.0	5.16
Pyrene	Pyr	129-00-0	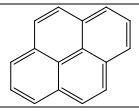	8.19	0.22	0.14	404.0±0.0	4.88
Benzo(a)anthracene	BaAnt	56-55-3	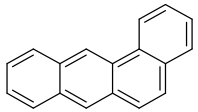	9.07	0.03	0.009	436.7±12.0	5.76
Chrysene	Chry	218-01-9	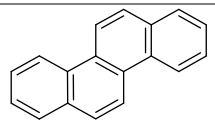	9.48	0.03	0.002	448.0±0.0	5.81

Benzo(b)fluoranthene	BbFlt	205-99-2	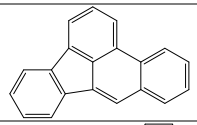	10.35	0.02	0.002	467.5±12.0	5.78
Benzo(k)fluoranthene	BaFlt	206-44-0	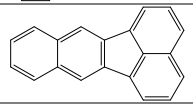	8.60	0.13	0.26	N.A.	5.16
Benzo(a)pyrene	BaPyr	50-32-8	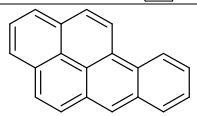	10.86	0.01	0.002	495.0±0.0	6.13
Indeno(1,2,3-cd)pyrene	IPyr	193-39-5	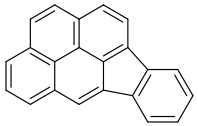	11.55	0.002	0.0002	497.1±12.0	6.70
Dibenzo(ah)anthracene	DBAnt	53-70-3	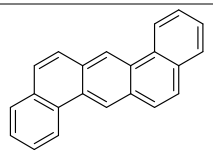	11.78	0.003	0.001	524.7±17.0	6.54
Benzo(g,h,i)perylene	BPer	191-24-2	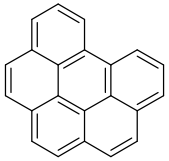	11.50	0.003	0.0003	501.0±0.0	6.63
1,4-Naphthoquinone	1,4-NapQ	130-15-4	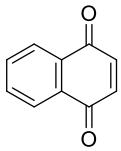	8.80	2417	N.A.	297.9±40.0	1.71
1-Nitronaphthalene	1-NNap	86-57-7	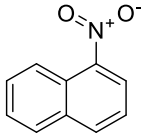	7.33	45.66	9.18	304.0±0.0	3.19
2-Nitronaphthalene	2-NNap	581-89-5	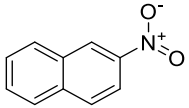	7.31	41.38	9.24	319.6±11.0	3.24

2-Nitrobiphenyl	2-NBip	086-00-0	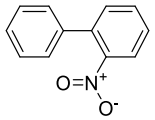	7.75	15.93	N.A.	325.0±11.0	3.57
9-Fluorenone	9-Flu	486-25-9	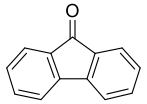	8.14	3.74	N.A.	341.5±0.0	3.58
4-Nitrobiphenyl	4-NBip	92-93-3	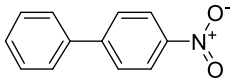	7.80	9.84	1.23	340.0±11.0	3.82
1,5-Dinitronaphthalene	1.5-DNNap	605-71-0	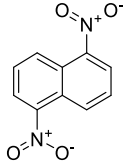	9.06	89.78	58.0	389.8±22.0	2.58
9,10-Anthraquinone	9.10-AntQ	84-65-1	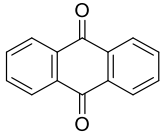	9.41	3.92	1.35	377.0±12.0	3.39
5-Nitroacenaphthene	5-NAce	602-87-9	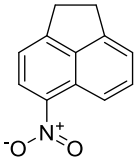	8.19	0.72	0.91	377.5±21.0	3.85
4H-Cyclopenta(def) phenanthrene-4-one	cPPhe-4	5737-13-3	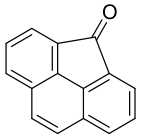	9.60	0.94	N.A.	411.6±12.0	4.14
2-Nitrofluorene	2-NFlu	607-57-8	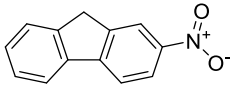	7.94	1.60	0.22	N.A.	3.37
9-Nitroanthracene	9-NAnt	602-60-8	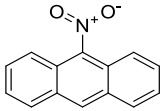	9.86	0.087	0.12	402.9±14.0	4.78

9,10-Phenanthrenequinone	9.10-PheQ	084-11-7	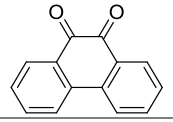	9.48	21.71	400.0	360.0±0.0	2.52
9-Nitrophenanthrene	9-NPhe	954-46-1	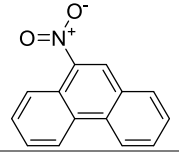	9.24	0.29	N.A.	413.3±14.0	4.16
3-Nitrophenanthrene	3-NPhe	17024-19-0	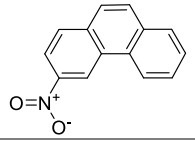	9.24	0.29	N. A.	423.9±14.0	4.16
2-Nitroanthracene	2-NAnt	3586-69-4	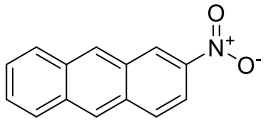	9.24	0.29	N.A.	423.9±14.0	4.16
Benzo(a)fluoren-11-one	BaFlu-11	479-79-8	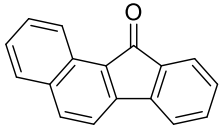	10.30	0.22	N.A.	431.7±12.0	4.73
Benzanthrone	BZT	82-05-3	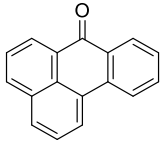	10.38	0.18	N.A.	436.2±12.0	4.81
2-Nitrofluoranthene	2-NFlt	13177-29-2	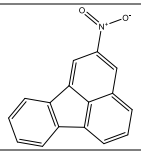	8.52	2.12	N.A.	N.A.	4.29
3-Nitrofluoranthene	3-NFlt	892-21-7	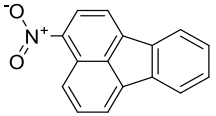	10.62	0.068	0.019	445.5±14.0	4.75

4-Nitropyrene	4-NPyr	57835-92-4	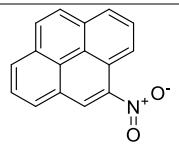	10.62	0.068	N.A.	445.5±14.0	4.75
Benzo(a)anthracene-7,12-dione	BaAnt-7,12	2498-66-0	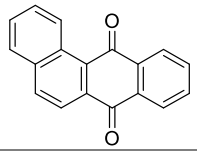	12.30	0.29	N.A.	472.5±15.0	4.40
1-Nitropyrene	1-NPyr	5522-43-0	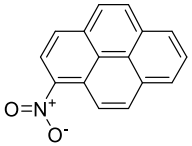	10.93	0.037	0.012	445.5±14.0	5.06
2,7-Dinitrofluorene	2.7-DNFlu	5405-53-8	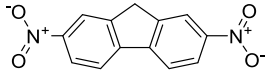	10.32	0.95	N.A.	451.5±38.0	3.35
7-Nitrobenz(a)anthracene	7-NBaAnt	20268-51-3	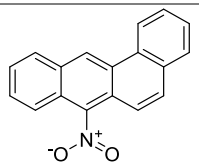	11.43	0.015	N.A.	495.3±14.0	5.34
6H-Benzo(cd)pyren-6-one	BPyr-6	3074-00-8	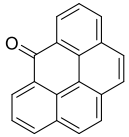	11.79	0.050	N.A.	509.5±17.0	5.31
6-Nitrochrysene	6-NChry	7496-02-8	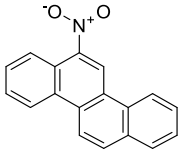	11.43	0.015	N.A.	505.0±19.0	5.34
1,3-Dinitropyrene	1.3-DNPyr	95713-52-3	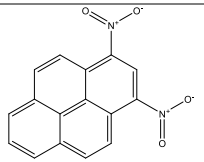	12.85	0.054	N.A.	493.9±25.0	4.57

1,6-Dinitropyrene	1.6-DNPyr	42397-64-8	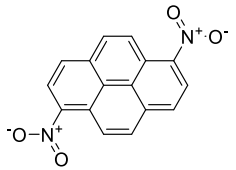	12.85	0.054	N.A.	515.2±30.0	4.57
1,8-Dinitropyrene	1.8-DNPyr	42397-65-9	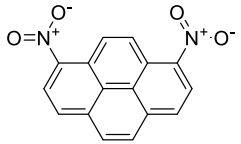	12.85	0.054	N.A.	515.2±30.0	4.57
6-Nitrobenzo(a)pyrene	6-NBaPyr	63041-90-7	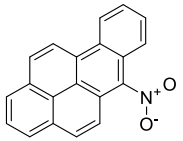	12.32	0.0091	N.A.	524.1±19.0	5.44

[1)] All structures were prepared with ChemDraw Professional, v 15.0.0.106, PerkinElmer Informatics, Inc., Boston, Massachusetts, USA, 2015

[2)] Acquired from EPI Suite, U.S.EPA: Estimation Programs Interface Suite, v 4.11, United States Environmental Protection Agency, Washington, DC, USA, 2019

[3)] Predicted data are calculated with ACD/Labs Percepta Platform − PhysChem Module, Toronto, Canada, 2015

210

Table S4. GC–EI-MS/MS parameters used for PAHs determination and instrumental limits of quantification (LOQ)

Compound	Retention time, min	Precursor ion, m/z	Product ion quantifier, m/z	Product ion qualifier, m/z	Collision energy, eV	LOQ, pg
Naphthalene-d8	**6.20**	**136**	**136**	**-**	**0**	**-**
Naphthalene	6.22	128	102	127	20/20	1.74
Acenaphtylene-d8	**7.88**	**160**	**160**	**-**	**0**	**-**
Acenaphtylene	7.89	152	151	150	25/25	1.29
Acenaphthene-d10	**8.07**	**164**	**164**	**-**	**0**	**-**
Acenaphthene	8.11	154	152	153	35/35	1.27
Fluorene-d10	**8.81**	**176**	**176**	**-**	**0**	**-**
Fluorene	8.86	166	165	164	40/40	1.14
Phenanthrene-d10	**10.46**	**188**	**188**	**-**	**0**	**-**
Phenanthrene	10.50	178	176	152	40/15	1.43
Anthracene-d10	**10.56**	**188**	**188**	**-**	**0**	**-**
Anthracene	10.56	178	176	152	40/15	1.56
Fluoranthnene-d10	**12.91**	**212**	**212**	**-**	**0**	**-**
Fluoranthnene	12.95	202	201	200	20/20	1.32
Pyrene-d10	**13.43**	**212**	**212**	**-**	**0**	**-**
Pyrene	13.47	202	201	200	20/20	0.98
Benzo(a)anthracene-d12	**16.78**	**240**	**240**	**-**	**0**	**-**
Benzo(a)anthracene	16.84	228	226	227	30/30	3.39
Chrysene-d12	**16.86**	**240**	**240**	**-**	**0**	**-**
Chrysene	16.94	228	226	227	30/30	2.92
Benzo(b+k)fluoranthene-d12	**20.45**	**264**	**264**	**-**	**0**	**-**
Benzo(b+k)fluoranthene	20.50	252	250	251	25/25	2.88
Benzo(a)pyrene-d12	**21.45**	**264**	**264**	**-**	**0**	**-**
Benzo(a)pyrene	21.52	252	250	251	25/25	2.95
Indeno(1,2,3-cd)pyrene-d12	**25.14**	**288**	**288**	**-**	**0**	**-**
Indeno(1,2,3-cd)pyrene	25.22	276	274	275	35/35	3.69
Dibenzo(a,h)anthracene-d12	**25.21**	**292**	**292**	**-**	**0**	**-**
Dibenzo(a,h)anthracene	25.30	278	276	277	25/25	3.54
Benzo(g,h,i)perylene-d14	**25.91**	**288**	**288**	**-**	**0**	**-**
Benzo(g,h,i)perylene	25.98	276	274	275	35/35	3.37

Table S5. GC-ECNI-MS parameters used for nitro- and oxy-PAHs determination and instrumental limits of quantification (LOQ)

Compound	Monitored ion, m/z	Retention time, min	LOQ, pg
1,4-Naphthaquinone-d6	**164**	**5.95**	-
1,4-Naphthaquinone	158	5.96	0.12
1-Nitronaphthalene-d7	**180**	**6.50**	-
1-Nitronaphthalene	173	6.60	0.09
2-Nitronaphthalene	173	6.90	0.09
2-Nitrobiphenyl-d9	**208**	**6.76**	-
2-Nitrobiphenyl	199	6.80	0.13
9-Fluorenone-d8	**188**	**6.90**	-
9-Fluorenone	180	7.00	0.49
4-Nitrobiphenyl	199	7.35	0.24
1,5-Dinitronaphtalene	218	7.60	0.23
Anthraquinone-d8	**216**	**7.80**	-
9,10-Anthraquinone	208	7.85	0.84
1,2,3,4-Tetrachloronaphthalene RSTD	**264**	**7.80**	-
5-Nitroacenaphthene	199	8.00	0.20
4H-Cyclopenta[def]phenanthrene-4-one	204	8.20	0.50
Fluoranthene-d10 RSTD	**212**	**8.30**	-
2-Nitrofluorene	211	8.50	0.26
2-Nitrofluorene-d9	**220**	**8.50**	-
9-Nitroanthracene-d9	**232**	**8.66**	-
9-Nitroanthracene	223	8.70	0.33
9,10-Phenanthrenequinone	208	8.95	26.87
9-Nitrophenanthrene	223	9.20	0.37
3-Nitrophenantherene	223	9.50	0.57
2-Nitroanthracene	223	9.90	0.58
Benzo[a]fluoren-11-one	230	10.40	0.75
Benzanthrone	230	11.90	2.69
3-Nitrofluoranthene-d9	**256**	**12.40**	-
2-Nitrofluoranthene	247	12.40	1.36
3-Nitrofluoranthene	247	12.50	1.22
4-Nitropyrene	247	12.70	1.12
Benzo[a]anthracene-7,12-dione	258	13.00	1.62
1-Nitropyrene-d9 RSTD	**256**	**13.20**	-
1-Nitropyrene	247	13.20	1.21
2-Nitropyrene	247	13.20	2.30
2,7-Dinitrofluorene	256	13.80	1.41
7-Nitrobenzo[a]anthracene	273	15.70	1.22
6H-Benzo[cd]pyren-6-one	254	16.50	5.35
6-Nitrochrysene-d11	**284**	**16.80**	-
6-Nitrochrysene	273	16.90	1.30
1,3-Dinitropyrene	292	17.80	1.27
1,6-Dinitropyrene	292	18.60	2.04
1,8-Dinitropyrene	292	19.10	1.55
6-Nitrobenzo(a)pyrene	297	21.00	1.14

220

Table S6. Blank values and method detection limits (MDL) for different sampling materials

	UNIS and Adventdalen				Power plant			
	QFF=7		PUF=7		QFF=7		PUF=7	
	Ø = 103 mm, Munktell**		L = 100 mm, Ziemer**		Ø = 47 mm, Pallflex**		L = 75 mm, Ziemer**	
Compound	Mean blank, pg	MDL*, pg	Mean blank, pg	MDL*, pg	Mean blank, pg	MDL*, pg	Mean blank, pg	MDL*, pg
Naphthalene	16394 ± 2765	24689	54223 ± 3648	65167	3849 ± 672	5865	33647 ± 5652	50603
Acenaphtylene	n.d.	-	272.1 ± 13.0	310.9	114.8 ± 10.0	144.9	1219.0 ± 231.6	1913.8
Acenaphthene	n.d.	-	307.9 ± 19.7	367.0	32.9 ± 3.9	44.6	211.4 ± 52.0	367.4
Fluorene	51.0 ± 6.6	70.8	6075 ± 508	7599	139.2 ± 9.5	167.7	3783 ± 677	5814
Phenanthrene	7660 ± 779	9997	43073 ± 2155	49538	394.8 ± 41.7	519.9	14051 ± 1731	19244
Anthracene	n.d.	-	n.d.	-	n.d.	-	630.0 ± 134.3	1032.9
Fluoranthene	274.2 ± 18.6	330.1	2389.4 ± 103.5	2699.9	61.9 ± 6.6	81.6	1597.5 ± 142.3	2024.4
Pyrene	259.7 ± 28.9	346.4	4369 ± 353	5428	183.6 ± 29.0	270.6	1089.8 ± 124.7	1463.9
Benzo(a)anthracene	n.d.	-	173.6 ± 13.4	213.7	n.d.	-	117.5 ± 22.0	183.5
Chrysene	77.4 ± 5.1	92.7	157.8 ± 10.7	189.9	n.d.	-	80.3 ± 11.1	113.7
Benzo(b+k)fluoranthene	n.d.	-	n.d.	-	n.d.	-	n.d.	-
Benzo(a)pyrene	n.d.	-	n.d.	-	n.d.	-	n.d.	-
Indeno(1,2,3-cd)pyrene	49.9 ± 5.0	64.9	n.d.	-	n.d.	-	86.8 ± 15.7	134.0
Dibenzo(a,h)anthracene	n.d.	-	n.d.	-	n.d.	-	n.d.	-
Benzo(g,h,i)perylene	53.9 ± 4.1	66.1	n.d.	-	n.d.	-	164.3 ± 27.0	245.3
1-Nitronaphthalene	24.4 ± 1.4	28.6	474.9 ± 24.5	548.4	707.4 ± 101.5	1011.9	238.4 ± 44.5	371.9
2-Nitronaphthalene	11.3 ± 1.3	15.1	255.0 ± 23.4	325.2	44.2 ± 6.9	65.0	94.7 ± 10.0	125
2-Nitrobiphenyl	4.3 ± 0.3	5.1	199.6 ± 16.4	248.7	48.3 ± 5.4	64.4	59.2 ± 9.9	89.0
9-Fluorenone	3453 ± 367	4554	15754 ± 1085	19009	1190.0 ± 152.4	1647.2	6486 ± 1275	10311
4-Nitrobiphenyl	n.d.	-	84.0 ± 7.6	106.8	n.d.	-	n.d.	-
1,5-Dinitronaphthalene	22.0 ± 1.7	27.2	152.2 ± 7.6	175.1	n.d.	-	204.1 ± 41.9	329.8
9,10-Anthraquinone	4399 ± 741	6622	10896 ± 724	13068	1106.8 ± 141.9	1532.5	3781 ± 718	5935
5-Nitroacenaphthene	n.d.	-	3.0 ± 3.4	44.2	n.d.	-	n.d.	-
cPPhen-4	695.0 ± 115.7	1042.1	1412.5 ± 110.4	1743.7	92.1 ± 9.7	121.3	446.0 ± 89.6	714.8
2-Nitrofluorene	12.0 ± 1.1	15.3	49.2 ± 3.7	60.3	149218 ± 17607	202039	39.0 ± 3.8	50.5
9-Nitroanthracene	64.1 ± 5.4	80.4	103.0 ± 6.1	121.2	n.d.	-	41.8 ± 4.5	55.4
9,10-Phenanthrenequinone	7799 ± 840	10319	3610 ± 280	4450	n.d.	-	2667 ± 379	3804
9-NPhe	258.4 ± 15.1	303.6	52.5 ± 4.9	67.2	n.d.	-	n.d.	-
3-Nitrophenanthrene	n.d.	-	n.d.	-	n.d.	-	26729 ± 4632	40625
2-Nitroanthracene	n.d.	-	n.d.	-	n.d.	-	85.5 ± 19.7	144.7
Benzo(a)fluoren-11-one	125.0 ± 9.5	153.5	n.d.	-	27.2 ± 3.1	36.5	50.1 ± 7.5	72.7
Benzanthrone	n.d.	-	135.6 ± 9.2	163.2	n.d.	-	179.1 ± 19.2	236.9
2+3-Nitrofluoranthene	1131.5 ± 169.3	1639.4	703.4 ± 58.9	880.1	n.d.	-	86.2 ± 14.0	128.4
4-Nitropyrene	n.d.	-	n.d.	-	n.d.	-	31.9 ± 5.0	47.0
Benzo(a)anthracene-7,12-dione	n.d.	-	n.d.	-	n.d.	-	n.d.	-
1-Nitropyrene	n.d.	-	n.d.	-	n.d.	-	n.d.	-
2,7-Dinitrofluorene	n.d.	-	n.d.	-	n.d.	-	n.d.	-
7-Nitrobenzo(a)anthracene	n.d.	-	n.d.	-	n.d.	-	139.4 ± 17.7	192.6
6H-Benzo(cd)pyren-6-one	n.d.	-	n.d.	-	n.d.	-	n.d.	-
6-Nitrochrysene	n.d.	-	n.d.	-	n.d.	-	n.d.	-

1,3-Dinitropyrene	n.d.	-	n.d.	-	n.d.	-	n.d.	-
1,6-Dinitropyrene	n.d.	-	n.d.	-	n.d.	-	n.d.	-
1,8-Dinitropyrene	n.d.	-	n.d.	-	n.d.	-	n.d.	-
6-Nitrobenzo(a)pyrene	n.d.	-	n.d.	-	n.d.	-	n.d.	-

* MDL = blank + 3*STD

** Sampling material with different size (PUF length or QFF diameter) and producers (Munktell, Ziemer, Pallflex) were used for air sampling

225

Table S7. Average recovery rates (Rec, %) and relative standard deviations (RSTD, %) for *spiked* samples

	Spiked QFF=4		Spiked PUF=4	
Compound	Mean Rec, %	RSTD, %	Mean Rec, %	RSTD, %
Nap	128.6 ± 10.0	7.8	121.2 ± 9.5	7.8
Acy	79.1 ± 6.8	8.6	93.3 ± 1.6	1.7
Ace	46.2 ± 4.2	9.1	48.0 ± 9.9	20.5
Flu	80.1 ± 9.1	11.3	109 ± 13.4	12.3
Phe	78.2 ± 9.4	12.0	83.7 ± 3.5	4.1
Ant	97.5 ± 4.6	4.7	119.8 ± 4.2	3.5
Flt	37.5 ± 5.4	14.3	43.5 ± 5.1	11.6
Pyr	80.9 ± 4.4	5.4	100.7 ± 2.3	2.3
BaAnt	77.6 ± 5.8	7.5	90.3 ± 4.3	4.8
Chry	78.9 ± 9.1	11.6	77.9 ± 5.8	7.4
BbkFlt	72.4 ± 10.1	13.9	90.9 ± 1.5	1.7
BaPyr	76.5 ± 5.1	6.6	86.0 ± 13.6	15.8
IPyr	75.6 ± 8.4	11.1	78.2 ± 5.7	7.3
DBAnt	86.9 ± 11.1	12.8	89.1 ± 2.1	2.3
BPer	81.1 ± 3.1	3.8	94.6 ± 10.0	10.6
dNap	64.5 ± 3.4	5.2	53.7 ± 11.0	20.4
dAcy	90.1 ± 9.5	10.6	73.0 ± 1.3	1.8
dAce	97.1 ± 8.7	9.0	89.4 ± 11.1	12.5
dFlu	68.9 ± 4.3	6.2	76.2 ± 9.3	12.2
dPhe	68.2 ± 16.4	24.0	82.4 ± 17.2	20.9
dAnt	111.3 ± 7.0	6.3	97.3 ± 5.3	5.4
dFlt	81.9 ± 10.9	13.3	100.4 ± 22.2	22.1
dPyr	107.8 ± 11.0	10.2	76.8 ± 5.0	6.5
dBaAnt	66.9 ± 9.0	13.4	82.6 ± 27.9	33.8
dChry	69.5 ± 9.7	13.9	80.1 ± 11.3	14.1
dBbkFlt	98.0 ± 7.1	7.3	100.6 ± 15.7	15.6
dBaPyr	98.9 ± 7.4	7.4	98.7 ± 5.9	6.0
dIPyr	102.2 ± 15.9	15.6	101.0 ± 17.6	17.5
dDBAnt	93.2 ± 8.4	9.0	89.8 ± 17.0	19.0
dBPer	96.9 ± 17.2	17.8	91.1 ± 9.2	10.1
1-Nnap	51.2 ± 10.9	21.2	72.3 ± 7.1	9.8
2-Nnap	61.4 ± 7.5	12.2	73.3 ± 19.5	26.6
2-NBip	74.4 ± 16.8	22.6	99.5 ± 9.9	9.9
9-Flu	40.1 ± 2.0	5.1	91.5 ± 7.7	8.4
4-NBip	65.9 ± 4.4	6.7	84.5 ± 18.3	21.7

1,5-DNNap	53.1 ± 8.4	15.9	69.0 ± 7.1	10.3
9,10-AntQ	42.0 ± 6.9	16.4	43.2 ± 4.4	10.3
5-NAce	74.3 ± 4.9	6.5	80.2 ± 10.0	12.5
cPPhe-4	44.1 ± 6.5	14.7	48.2 ± 2.4	4.9
2-Nflu	66.6 ± 5.0	7.6	66.3 ± 14.9	22.4
9-Nant	42.5 ± 16.7	39.3	78.0 ± 6.7	8.5
9,10-PheQ	56.8 ± 10.2	18.0	74.0 ± 7.6	10.3
9-NPhe	64.2 ± 6.0	9.3	104.7 ± 15.6	14.8
3-Nphe	65.7 ± 8.4	12.9	87.7 ± 4.9	5.5
2-Nant	46.2 ± 11.6	25.1	107.1 ± 11.0	10.3
BaFlu-11	47.4 ± 3.0	6.3	109.5 ± 20.4	18.6
BZT	37.8 ± 7.2	19.0	43.8 ± 3.1	7.1
2+3-NFlt	59.3 ± 15.4	25.9	79.6 ± 13.5	17.0
4-Npyr	54.6 ± 5.7	10.4	79.2 ± 10.3	13.0
BaAnt-7,12	46.8 ± 12.1	25.8	69.4 ± 4.0	5.8
1-Npyr	49.1 ± 15.5	31.5	56.2 ± 7.9	14.0
7-NBaAnt	69.8 ± 35.2	50.4	100.4 ± 8.5	8.5
BPyr-6	2.0 ± 0.3	13.7	4.1 ± 0.2	5.0
6-Nchry	58.8 ± 5.3	8.9	83.5 ± 8.3	9.9
1,3-DNPyr	17.8 ± 3.0	17.0	104.4 ± 36.8	35.2
1,6-DNPyr	22.6 ± 1.0	4.2	98.6 ± 17.9	18.2
1.8-DNPyr	9.5 ± 0.3	3.2	50.0 ± 12.3	24.5
6-NBaPyr	6.4 ± 0.5	7.1	32.6 ± 7.0	21.5
1-NNap-d7	60.7 ± 1.1	1.7	73.3 ± 9.2	12.5
2-NBP-d9	77.1 ± 3.9	5.1	104.1 ± 12.6	12.1
9-Flu-d8	40.7 ± 5.7	13.9	73.8 ± 8.8	12.0
AntQ-d8	39.6 ± 3.4	8.5	50.3 ± 8.6	17.2
2-NFlu-d9	68.6 ± 9.7	14.2	73.5 ± 6.6	8.9
9-NAnt-d9	39.9 ± 3.4	8.6	69.0 ± 8.3	12.0
3-NFlt-d9	55.3 ± 7.6	13.7	79.6 ± 14.4	18.1
6-NChry-d11	59.4 ± 1.2	2.1	93.1 ± 16.2	17.4

Table S8. Average recovery rates (Rec, %) of internal standards (ISTDs) for *ambient air* samples

ISTD	Rec, %	Rec, %
	QFF=15	PUF=15
dNap	68.6 ± 11.2	68.4 ± 6.2
dAcy	70.7 ± 7.8	99.1 ± 22.3
dAce	100.2 ± 27.5	74.4 ± 17.9
dFlu	90.8 ± 9.2	76.9 ± 25.8
dPhe	66.3 ± 5.8	100.8 ± 15.9
dAnt	63.3 ± 11.3	91.7 ± 33.0
dFlt	68.6 ± 5.2	93.9 ± 15.8
dPyr	102.4 ± 6.1	84.3 ± 11.6
dBaAnt	94.8 ± 12.6	103.5 ± 21.3
dChry	63.9 ± 7.6	83.2 ± 18.7
dBbkFlt	99.8 ± 15.4	99.3 ± 6.4
dBaPyr	74.9 ± 6.0	97.5 ± 17.0
dIPyr	72.0 ± 4.9	109.1 ± 20.0
dDBAnt	80.1 ± 22.6	101.3 ± 13.1
dBPer	91.1 ± 14.3	79.3 ± 12.9
1-NNap-d7	59.8 ± 3.7	80.3 ± 23.7
2-NBP-d9	70.0 ± 8.0	89.0 ± 4.3
9-Flu-d8	60.6 ± 16.6	67.7 ± 4.3
9,10-AntQ-d8	56.2 ± 12.4	69.0 ± 20.9
2-NFlu-d9	52.7 ± 6.0	84.5 ± 18.1
9-NAnt-d9	74.5 ± 14.8	65.2 ± 6.7
3-NFlt-d9	63.1 ± 5.7	49.3 ± 7.4
6-NChry-d11	44.0 ± 7.7	49.1 ± 9.0

230

Table S9. Concentrations of PAHs (G+P) and percentage in the particulate phase (%PM) in *Longyearbyen power plant* (n=6), as well as MDLs for gaseous (PUF) and particulate (QFF) phases, and instrumental LOD and LOQ; all values are in pg m^{-3}*

Variable	Mean conc ± STD, pg m^{-3}	Median pg m^{-3}	Min – Max pg m^{-3}	Mean %PM	MDL_{QFF} pg m^{-3}	MDL_{PUF} pg m^{-3}	LOD pg m^{-3}	LOQ pg m^{-3}
Naphthalene	51817.0 ± 10297.0	55629.0	32737.0 - 59824.0	7.4	1515.2	23992.0	0.3	0.9
Acenaphtylene	2301.0 ± 1059.0	2203.0	1218.0 - 3797.0	0.6	107.9	1024.0	0.2	0.6
Acenaphthene	873.0 ± 778.0	487.0	300.0 - 2177.0	8.4	29.5	145.2	0.2	0.6
Fluorene	7607.0 ± 3568.0	6946.0	3680.0 - 12164.0	4.6	62.3	3445.5	0.2	0.6
Phenanthrene	27324.0 ± 12700.0	27530.0	12015.0 - 44871.0	5.6	159.2	9242.6	0.2	0.7
Anthracene	1055.0 ± 818.0	925.0	229.2 - 2136.0	0.0	n.d.	458.4	0.3	0.8
Fluoranthene	6991.0 ± 3754.0	6961.0	1428.0 - 12494.0	3.9	47.7	1126.6	0.2	0.7
Pyrene	4404.0 ± 2178.0	4700.0	1083.0 - 7348.0	8.3	75.2	717.9	0.2	0.5
Benzo(a)anthracene	130.7 ± 77.3	156.7	36.4[2)] - 202.8	0.0	n.d.	72.9	0.6	1.7
Chrysene	277.3 ± 141.4	333.3	60.7 - 421.3	0.0	n.d.	54.7	0.5	1.4
Benzo(b+k)fluoranthene	n.d.	n.d.	n.d.	-	n.d.	n.d.	0.5	1.4
Benzo(a)pyrene	n.d.	n.d.	n.d.	-	n.d.	n.d.	0.5	1.5
Indeno(1,2,3-cd)pyrene	n.d.	n.d.	n.d.	-	n.d.	132.2	0.6	1.8
Dibenzo(a,h)anthracene	n.d.	n.d.	n.d.	-	n.d.	n.d.	0.6	1.8
Benzo(g,h,i)perylene	n.d.	n.d.	n.d.	-	n.d.	225.4	0.6	1.7
1-Nitronaphthalene	2188.0 ± 1341.0	1729.0	988.0 - 4685.0	61.7	241.0	158.9	0.0	0.0
2-Nitronaphthalene	257.3 ± 108.8	273.6	105.9 - 395.1	31.7	20.3	74.9	0.0	0.0
2-Nitrobiphenyl	157.4 ± 75.7	154.2	69.2 - 290.3	39.9	18.8	38.8	0.0	0.1
9-Fluorenone	12352.0 ± 5258.0	11937.0	5566.0 - 19541.0	19.2	479.0	4368.6	0.1	0.2
4-Nitrobiphenyl	n.d.	n.d.	n.d.	-	n.d.	n.d.	0.0	0.1
1,5-Dinitronaphthalene	n.d.	n.d.	n.d.	-	n.d.	139.7	0.0	0.1
9,10-Anthraquinone	15758.0 ± 15578.0	10806.0	4595.0 - 46956.0	21.3	446.8	2558.7	0.1	0.4
5-Nitroacenaphthene	n.d.	n.d.	n.d.	-	n.d.	n.d.	0.0	0.1
cPPhen-4	1304.0 ± 743.0	1320.0	506.0 - 2554.0	15.8	39.3	326.7	0.1	0.2
2-Nitrofluorene	42.5 ± 54.3	25.0	22.0[2)] - 134.5	0.0	777.5	44.0	0.0	0.1
9-Nitroanthracene	79.6 ± 77.2	61.4	20.5[2)] - 226.7	0.0	n.d.	41.1	0.1	0.2
9,10-Phenanthrenequinone	2127.0 ± 1934.0	2061.0	960.1[2)] - 4400.0	0.0	n.d.	1920.2	9.4	28.3
9-Nitrophenanthrene	n.d.	n.d.	n.d.	-	n.d.	n.d.	0.1	0.2
3-Nitrophenanthrene	761.0 ± 757.0	656.0	0.3[1)] - 1930.0	96.1	n.d.	76.0	0.1	0.3
2-Nitroanthracene	305.7 ± 235.5	261.4	66.1[2)] - 620.9	0.0	n.d.	132.2	0.1	0.3
Benzo(a)fluoren-11-one	157.5 ± 55.2	165.0	75.5 - 227.0	27.6	27.0	32.9	0.1	0.4
Benzanthrone	866.0 ± 418.0	920.0	135.0 - 1314.0	0.0	n.d.	117.1	0.4	1.3
2+3-Nitrofluoranthene	519.3 ± 437.1	442.1	61.0 - 1140.3	0.0	n.d.	53.6	0.2	0.6
4-Nitropyrene	114.8 ± 70.0	151.5	25.7[2)] - 174.5	0.0	n.d.	51.4	0.2	0.6
Benzo(a)anthracene-7,12-dione	n.d.	n.d.	n.d.	-	n.d.	n.d.	0.3	0.8
1-Nitropyrene	n.d.	n.d.	n.d.	-	n.d.	n.d.	0.2	0.6
2,7-Dinitrofluorene	58.8 ± 53.1	70.5	0.6[1)] - 141.0	0.0	n.d.	n.d.	0.2	0.6
7-Nitrobenzo(a)anthracene	578.0 ± 376.0	709.0	114.2[2)] - 932.0	0.0	n.d.	228.5	0.2	0.6
6H-Benzo(cd)pyren-6-one	n.d.	n.d.	n.d.	-	n.d.	n.d.	0.9	2.6
6-Nitrochrysene	n.d.	n.d.	n.d.	-	n.d.	n.d.	0.2	0.6
1,3-Dinitropyrene	n.d.	n.d.	n.d.	-	n.d.	n.d.	0.2	0.6
1,6-Dinitropyrene	n.d.	n.d.	n.d.	-	n.d.	n.d.	0.3	1.0
1,8-Dinitropyrene	n.d.	n.d.	n.d.	-	n.d.	n.d.	0.3	0.8
6-Nitrobenzo(a)pyrene	n.d.	n.d.	n.d.	-	n.d.	n.d.	0.2	0.6
∑PAHs	102846 ± 31931		61925 - 139082					
∑oxy-PAHs	32565 ± 20963		15767 - 73084					
∑nitro-PAHs	4451 ± 2075		2046 - 7752					

* LOD, LOQ and MDL in pg (Tables S4-S6) were converted to pg m^{-3} using 2 m^3 as average sample volume
n.d. not detected

[1)] equal LOQ

[2)] ½ of MDL

Table S10. Concentrations of PAHs (G+P) and percentage in the particulate phase (%PM) at *UNIS* (n=6), as well as MDLs for gaseous (PUF) and particulate (QFF) phases, and instrumental LOD and LOQ; all values are in pg m^{-3}*

Variable	Mean conc ± STD, pg m^{-3}	Median pg m^{-3}	Min – Max pg m^{-3}	Mean %PM ± STD	MDL qff pg m^{-3}	MDL puf pg m^{-3}	LOD pg m^{-3}	LOQ pg m^{-3}
Naphthalene	< MDL	< MDL	< MDL	-	45.6	241.8	0.002	0.005
Acenaphtylene	16.9 ± 8.2	16.6	7.1 - 29.2	0 ± 0.0	n.d.	0.8	0.001	0.003
Acenaphthene	48.5 ± 20.5	45.7	24.3 - 73.0	0 ± 0.0	n.d.	0.9	0.001	0.003
Fluorene	170.5 ± 39.6	155.2	136.5 - 236.0	1.1 ± 1.0	0.2	26.6	0.001	0.003
Phenanthrene	409.2 ± 34.3	401.8	368.5 - 470.0	6.5 ± 8.6	32.4	179.6	0.001	0.004
Anthracene	18.0 ± 4.5	17.2	12.3 - 25.5	0 ± 0.0	n.d.	n.d.	0.001	0.004
Fluoranthene	28.5 ± 4.3	27.5	24.1 - 36.1	40.5 ± 19.4	1.2	7.4	0.001	0.004
Pyrene	39.5 ± 6.3	37.9	30.7 - 47.8	26.8 ± 18.6	1.1	12.7	0.001	0.003
Benzo(a)anthracene	2.2 ± 2.6	1.2	0.009[1)] - 5.8	68.2 ± 2.4	n.d.	0.5	0.003	0.009
Chrysene	7.3 ± 4.3	6.6	2.6 - 13.5	81.7 ± 10.3	0.2	0.4	0.003	0.008
Benzo(b+k)fluoranthene	2.2 ± 2.1	1.8	0.008[1)] - 5.9	100 ± 0.0	n.d.	n.d.	0.003	0.008
Benzo(a)pyrene	0.9 ± 1.1	0.6	0.008[1)] - 2.5	100 ± 0.0	n.d.	n.d.	0.003	0.008
Indeno(1,2,3-cd)pyrene	1.6 ± 1.5	1.8	0.07[2)] - 3.8	100 ± 0.0	0.15	n.d.	0.003	0.010
Dibenzo(a,h)anthracene	n.d.	n.d.	n.d.	-	n.d.	n.d.	0.003	0.009
Benzo(g,h,i)perylene	3.9 ± 2.5	3.7	1.4 - 8.1	100 ± 0.0	0.2	n.d.	0.003	0.009
1-Nitronaphthalene	17.0 ± 3.0	16.4	13.4 - 21.5	0.1 ± 0.2	0.1	1.3	0.000	0.001
2-Nitronaphthalene	5.1 ± 2.0	5.1	2.4 - 7.3	3.1 ± 5.6	0.04	1.0	0.000	0.001
2-Nitrobiphenyl	1.0 ± 0.1	1.0	0.8 - 1.2	10.1 ± 8.3	0.01	0.6	0.000	0.001
9-Fluorenone	270.3 ± 146.9	211.2	128.2 - 543.8	41.7 ± 22.3	14.1	62.1	0.001	0.004
4-Nitrobiphenyl	2.2 ± 0.5	2.4	1.5 - 2.7	0 ± 0.0	n.d.	0.2	0.001	0.002
1,5-Dinitronaphthalene	0.8 ± 0.9	0.5	0.05 - 2.2	80.0 ± 44.7	0.1	0.4	0.001	0.002
9,10-Anthraquinone	163.5 ± 57.4	159.6	105.2 - 269.1	37.5 ± 22.4	19.3	22.8	0.002	0.007
5-Nitroacenaphthene	0.2 ± 0.1	0.2	0.05[2)] - 0.38	-	n.d.	0.1	0.001	0.002
cPPhen-4	27.2 ± 6.9	25.1	20.2 - 35.8	65.5 ± 10.6	2.8	5.1	0.001	0.004
2-Nitrofluorene	0.2 ± 0.3	0.1	0.07[2)] - 0.8	15.1 ± 7.5	0.04	0.15	0.001	0.002
9-Nitroanthracene	0.6 ± 0.3	0.7	0.2[2)] - 0.9	-	0.2	0.4	0.001	0.003
9,10-Phenanthrenequinone	< MDL	< MDL	< MDL	-	22.5	14.4	0.155	0.464
9-Nitrophenanthrene	0.2 ± 0.2	0.3	0.1[2)] - 0.4	-	1.1	0.2	0.001	0.003
3-Nitrophenanthrene	n.d.	n.d.	n.d.	-	n.d.	n.d.	0.002	0.005
2-Nitroanthracene	n.d.	n.d.	n.d.	-	n.d.	n.d.	0.002	0.005
Benzo(a)fluoren-11-one	6.1 ± 3.6	5.0	1.8 - 11.1	100 ± 0.0	0.6	n.d.	0.002	0.006
Benzanthrone	1.8 ± 1.8	1.7	0.02[1)] - 4.3	96.7 ± 4.8	n.d.	0.5	0.007	0.022
2+3-Nitrofluoranthene	9.5 ± 1.6	9.7	7.3 - 11.4	94.5 ± 13.5	4.5	2.1	0.003	0.010
4-Nitropyrene	n.d.	n.d.	n.d.	-	n.d.	n.d.	0.003	0.009
Benzo(a)anthracene-7,12-dione	2.2 ± 1.8	2.2	0.01[1)] - 4.9	100 ± 0.0	n.d.	n.d.	0.004	0.013
1-Nitropyrene	n.d.	n.d.	n.d.	-	n.d.	n.d.	0.003	0.010
2,7-Dinitrofluorene	n.d.	n.d.	n.d.	-	n.d.	n.d.	1.003	3.010
7-Nitrobenzo(a)anthracene	n.d.	n.d.	n.d.	-	n.d.	n.d.	0.003	0.010
6H-Benzo(cd)pyren-6-one	n.d.	n.d.	n.d.	-	n.d.	n.d.	0.014	0.043
6-Nitrochrysene	n.d.	n.d.	n.d.	-	n.d.	n.d.	0.004	0.011
1,3-Dinitropyrene	n.d.	n.d.	n.d.	-	n.d.	n.d.	0.003	0.010
1,6-Dinitropyrene	n.d.	n.d.	n.d.	-	n.d.	n.d.	0.006	0.017
1,8-Dinitropyrene	n.d.	n.d.	n.d.	-	n.d.	n.d.	0.004	0.013
6-Nitrobenzo(a)pyrene	n.d.	n.d.	n.d.	-	n.d.	n.d.	0.003	0.009
∑PAHs	749.2 ± 72.6		687.4 - 866.9					
∑oxy-PAHs	471.0 ± 150.8		325.9 - 741.4					
∑nitro-PAHs	36.76 ± 6.19		30.30 - 46.10					

* LOD, LOQ and MDL in pg (Tables S4-S6) were converted to pg m^{-3} using 370 m^3 as average sample volume

<MDL below method detection limit

n.d. not detected

[1)] equal LOQ

[2)] ½ of MDL

Table S11. Concentrations of PAHs (G+P) and percentage in the particulate phase (%PM) at *Adventdalen* (n=6), as well as MDLs for gaseous (PUF) and particulate (QFF) phases, and instrumental LOD and LOQ; all values are in pg m^{-3}*

Variable	Mean conc ± STD, pg m^{-3}	Median pg m^{-3}	Min – Max pg m^{-3}	Mean %PM ± STD	MDL qff pg m^{-3}	MDL puf pg m^{-3}	LOD pg m^{-3}	LOQ pg m^{-3}
Naphthalene	< MDL	< MDL	< MDL	-	45.6	241.8	0.002	0.005
Acenaphtylene	2.4 ± 1.5	2.1	1.1 - 5.1	0 ± 0	-	0.8	0.001	0.004
Acenaphthene	3.8 ± 2.5	3.8	1.3 - 6.6	0 ± 0	-	0.9	0.001	0.003
Fluorene	60.0 ± 23.2	50.1	38.5 - 95.8	1.8 ± 3.0	0.2	26.6	0.001	0.003
Phenanthrene	236.3 ± 31.8	236.2	191.7 - 270.8	3.7 ± 9.0	32.4	179.6	0.001	0.004
Anthracene	14.3 ± 3.4	13.9	10.5 - 19.3	3.5 ± 8.5	-	-	0.001	0.004
Fluoranthene	19.1 ± 10.0	15.8	10.8 - 38.5	23.2 ± 9.2	1.2	7.4	0.001	0.004
Pyrene	27.2 ± 6.4	26.4	20.9 - 35.9	15.8 ± 11.0	1.1	12.7	0.001	0.003
Benzo(a)anthracene	n.d.	n.d.	n.d.	-	-	0.5	0.003	0.009
Chrysene	3.1 ± 2.5	2.7	0.1[1)] - 7.1	64.1 ± 18.7	0.2	0.4	0.003	0.008
Benzo(b+k)fluoranthene	0.7 ± 1.2	0.0	0.008[1)] - 2.785	100 ± 0	-	-	0.003	0.008
Benzo(a)pyrene	0.3 ± 0.5	0.0	0.008[1)]- 1.163	100 ± 0	-	-	0.003	0.008
Indeno(1,2,3-cd)pyrene	0.7 ± 1.2	0.0	0.07[2)] - 2.67	100 ± 0	0.15	-	0.003	0.010
Dibenzo(a,h)anthracene	n.d.	n.d.	n.d.	-	-	-	0.003	0.010
Benzo(g,h,i)perylene	1.2 ± 1.5	0.8	0.08[2)] - 3.83	100 ± 0	0.2	-	0.003	0.009
1-Nitronaphthalene	5.0 ± 3.2	4.2	1.9 - 9.8	1.5 ± 3.6	0.1	1.3	0.000	0.001
2-Nitronaphthalene	1.9 ± 0.6	1.7	1.3 - 2.8	5.4 ± 8.0	0.1	1.0	0.000	0.001
2-Nitrobiphenyl	1.0 ± 0.2	0.9	0.8 - 1.3	5.9 ± 10.0	0.1	0.6	0.000	0.001
9-Fluorenone	139.4 ± 24.9	137.3	110.2 - 177.2	25.5 ± 13.4	14.1	62.1	0.001	0.004
4-Nitrobiphenyl	2.5 ± 1.2	2.6	0.3 - 4.1	-	-	0.2	0.001	0.002
1,5-Dinitronaphthalene	0.9 ± 1.4	0.6	0.05[2)] - 3.72	53.9 ± 53.6	0.1	0.4	0.001	0.002
9,10-Anthraquinone	71.7 ± 39.2	80.3	11.4[2)] - 118.4	43.9 ± 1.4	19.3	22.8	0.002	0.007
5-Nitroacenaphthene	0.3 ± 0.7	0.0	0.05[2)] - 1.62	-	-	0.1	0.001	0.002
cPPhen-4	18.8 ± 10.2	15.1	12.0 - 39.1	38.1 ± 20.2	2.8	5.1	0.001	0.004
2-Nitrofluorene	0.6 ± 0.4	0.7	0.07[2)] - 1.05	4.2 ± 9.5	0.15	0.1	0.001	0.002
9-Nitroanthracene	2.3 ± 1.9	1.8	1.0 - 4.7	57.8 ± 29.7	0.2	0.4	0.001	0.003
9,10-Phenanthrenequinone	n.d.	n.d.	n.d.	-	22.5	14.4	0.155	0.464
9-Nitrophenanthrene	0.4 ± 0.4	0.4	0.09[2)] - 1.17	25 ± 50	1.1	0.2	0.001	0.003
3-Nitrophenanthrene	n.d.	n.d.	n.d.	-	-	-	0.002	0.005
2-Nitroanthracene	n.d.	n.d.	n.d.	-	-	-	0.002	0.005
Benzo(a)fluoren-11-one	2.2 ± 1.7	1.6	0.7 - 4.4	100 ± 0	0.6	-	0.002	0.006
Benzanthrone	0.1 ± 0.2	0.0	0.02[1)] - 0.58	100 ± 0	-	0.5	0.007	0.022
2+3-Nitrofluoranthene	12.3 ± 7.7	9.8	4.7 - 26.7	79.8 ± 16.5	4.5	2.1	0.003	0.010
4-Nitropyrene	n.d.	n.d.	n.d.	-	-	-	0.003	0.009
Benzo(a)anthracene-7,12-dione	0.9 ± 0.7	0.7	0.01[1)] - 2.21	100 ± 0	-	-	0.004	0.013
1-Nitropyrene	n.d.	n.d.	n.d.	-	-	-	0.003	0.010
2,7-Dinitrofluorene	n.d.	n.d.	n.d.	-	-	-	1.003	3.010
7-Nitrobenzo(a)anthracene	n.d.	n.d.	n.d.	-	-	-	0.003	0.010
6H-Benzo(cd)pyren-6-one	n.d.	n.d.	n.d.	-	-	-	0.015	0.043
6-Nitrochrysene	n.d.	n.d.	n.d.	-	-	-	0.004	0.011
1,3-Dinitropyrene	n.d.	n.d.	n.d.	-	-	-	0.003	0.010
1,6-Dinitropyrene	n.d.	n.d.	n.d.	-	-	-	0.006	0.017
1,8-Dinitropyrene	n.d.	n.d.	n.d.	-	-	-	0.004	0.013
6-Nitrobenzo(a)pyrene	n.d.	n.d.	n.d.	-	-	-	0.003	0.009
∑PAHs	369.1 ± 66.7		279.0 - 454.5					
∑oxy-PAHs	233.1 ± 68.3		124.7 - 337.1					
∑nitro-PAHs	27.16 ± 11.14		13.50 - 44.43					

* LOD, LOQ and MDL in pg (Tables S4-S6) were converted to pg m^{-3} using 370 m^3 as average sample volume

<MDL below method detection limit

n.d. not detected

[1)] equal LOQ

[2)] ½ of MDL

Table S12. Comparison of Longyearbyen power plant 16 PAH emissions with other coal-burning plants operated worldwide

Power plant	Location	Coal type	Boiler capacity, conditions	Flue gas cleaning	Dust in flue gas, mg m^{-3}	EF, µg kg^{-1}	∑PAHs, µg m^{-3}	%PM	Predominant PAHs	PAH profile	References
Energyverket	Longyearbyen, Svalbard	Bituminous, Ro=0.78%, High volatile	68 ton-coal/day, two boilers 32 MW each	SNCR+ESP+WFGD	1.5	1.5	0.106	0.06	Nap+ Phe+ Flu, Flt+ Pyr	53% 2 rings, 36 % 3 rings, 11% 4 rings 5-6 rings n.d.	This work
n.a.	Central Taiwan	Indonesian and Australian	6480 ton-coal/day	SCR+ESP+FGD	6.0	1.5	0.268	n.a.	Nap + Phe, Flt, Pyr + Flu	45% 2 rings, 20 % 3 rings, 30% 4 rings, 5% rest	(Hsu et al., 2016)
Fusina plant	Porto Marghera, Italy	n.a.	n.a.	SCR + ESP + FGD	5.2	n.a.	0.697	n.a.	n.a.	n.a.	(Rigamonti et al., 2012)
n.a.	Netherlands	From different countries	n.a.	ESP+FGD	n.a.	n.a.	1-3	n.a.	n.a.	n.a.	(Meij and Te Winkel, 2007)
Point F	China	Blend	1000 MW	SCR + LLT-ESP + WFGD	4.0	n.a.	5.255	0.09	Nap+ Phe + 6 rings	80% 2 rings	(Li et al., 2016)
Point G	China	Blend	1000 MW	SCR + LLT-ESP + WFGD + WESP	< 1.9	n.a.	0.870	0.51	5 and 6 rings, no Nap	73% 5 and 6 rings	(Li et al., 2016)
HPA-3	Huainan, China	Bituminous	600 MW	ESP + WFGD	10.4	n.a.	11.67	0.39	Nap + Acy, Ant, Phe	n.a.	(Wang et al., 2015)
HPB-2	Huainan, China	Bituminous	600 MW	ESP + WFGD	10.6	n.a.	11.87	0.30	Nap + Acy, Flu	n.a.	(Wang et al., 2015)
HPC-1	Huainan, China	Bituminous	600 MW	ESP + WFGD	11.2	n.a.	8.84	0.32	Nap + Acy, Ant	n.a.	(Wang et al., 2015)

n.a. not available

SCR is selective catalytic reduction system; SNCR is selective non-catalytic reduction system

ESP is electrostatic precipitator; LLT-ESP is low-low temperature ESP

FGD is flue-gas desulfurization scrubber; WFGD is wet FGD

Table S13. UNIS and Adventdalen air concentrations (G+P) of 16 PAHs compared to national and regional background concentrations detected in *autumn 2018*

Components	UNIS (ng m^{-3})[2)]			Adventdalen (ng m^{-3})[2)]			Birkenes (ng m^{-3})[1,3)]			Zeppelin (ng m^{-3})[1,4)]		
	Average	Min	Max	Average	Min	Max	Average	Min	Max	Average	Min	Max
Naphthalene	n.q.	n.q.	n.q.	n.q.	n.q.	n.q.	0.034	0.028	0.044	0.094[5)]	0.081	0.107
Acenaphthylene	0.017	0.007	0.029	0.002	0.001	0.002	0.019	0.002	0.052	n.d.	n.d.	n.d.
Acenaphthene	0.049	0.024	0.073	0.004	0.001	0.007	0.141	0.027	0.301	0.002	0.002	0.002
Fluorene	0.171	0.137	0.236	0.060	0.039	0.096	0.264	0.172	0.334	0.009	0.001	0.014
Phenanthrene	0.409	0.369	0.470	0.236	0.192	0.271	0.675	0.508	0.878	0.009	0.005	0.016
Anthracene	0.018	0.012	0.026	0.014	0.011	0.019	0.009	0.003	0.030	0.001	0.001	0.001
Fluoranthene	0.029	0.024	0.036	0.019	0.011	0.039	0.141	0.113	0.193	0.004	0.003	0.004
Pyrene	0.040	0.031	0.048	0.027	0.021	0.036	0.081	0.055	0.100	0.003	0.002	0.004
Benzo(a)anthracene	0.002	9.0E-06	0.006	n.d.	n.d.	n.d.	0.006	0.003	0.010	n.d.	n.d.	n.d.
Chrysene	0.007	0.003	0.014	0.003	1.00E-04	0.007	0.052	0.025	0.084	n.d.	n.d.	n.d.
Benzo(b+k)fluoranthene	0.002	7.0E-06	0.006	0.001	8.00E-06	0.003	0.050	0.015	0.104	n.d.	n.d.	n.d.
Benzo(a)pyrene	0.001	7.0E-06	0.002	3.00E-04	8.00E-06	0.001	0.004	0.002	0.009	n.d.	n.d.	n.d.
Indeno(123-cd)pyrene	0.002	7.4E-05	0.004	0.001	7.00E-05	0.003	0.014	0.006	0.020	n.d.	n.d.	n.d.
Dibenzo(ah)anthracene	n.d.	n.d.	n.d.	n.d.	n.d.	n.d.	0.004	0.002	0.007	n.d.	n.d.	n.d.
Benzo(ghi)perylene	0.004	0.001	0.008	0.001	8.00E-05	0.004	0.020	0.009	0.029	n.d.	n.d.	n.d.

n.d.: below detection limits
n.q.: high blank contamination
[1)] Data acquired from http://ebas.nilu.no, last access: 20 June 2020
[2-4)] Volume sampled: 350-450 m^3, 650 m^3, and 1300 m^3, respectively
[5)] Possibly influenced by blank levels
NOTE the chemical profiles are presented as Figure S3

Table S14: Comparison of average concentrations (G+P; pg m^{-3}) of PAHs, oxy-PAHs and nitro-PAHs measured in Longyearbyen with those previously reported in the literature for rural sites worldwide

Region	Season	Sampling phase	Type of site	Number of compared compounds*	Average sum concentration (pg m^{-3})	Reference
Parent PAHs						
France, Marseille	Summer 2004	G+P	Rural	13	15959	(Albinet et al., 2007)
Denmark, Risø	Winter 1998	P	Semi-rural	9	4390	(Feilberg et al., 2001)
Eastern England, Weybourne	Winter 2010	G+P	Background	12	2298	(Alam et al., 2014)
Southern China, Wanqingsha	Autumn 2010	G+P	Background	15	88950	(Huang et al., 2014b)
Subarctic, Finland, Pallas	Autumns 1996-2015	G+P	Background	12	403	(Yu et al., 2019)
Arctic, Canada, Alert	Autumns 1992-2015	G+P	Background	15	81	(Yu et al., 2019)
Arctic, Svalbard, Zeppelin	Autumns 1994-2015	G+P	Background, altitude	13	185	(Yu et al., 2019)
Southern Norway, Birkenes	Autumn 2018	G+P	Background	15	1480	(NILU, 2018)
Arctic, Svalbard, Zeppelin	Autumn 2018	G+P	Background, altitude	15	28	(NILU, 2018)
Arctic, Svalbard, UNIS	Autumn 2018	G+P	Semi-urban	15	749	This study
Arctic, Svalbard, Adventdalen	Autumn 2018	G+P	Rural	15	369	This study
Nitro-PAHs						
Northern China	Annual 2010-2011	G+P	Rural	12	**911	(Li et al., 2015)
Southern China, Wanqingsha	Autumn 2010	G+P	Rural	23	4021	(Huang et al., 2014b)
France, Marseille	Summer 2004	G+P	Rural	9	26	(Albinet et al., 2007)
France, The Alps, Chamonix	Winter 2002	P	Rural, altitude	10	9	(Albinet et al., 2008a)
France, The Alps, Maurienne	Winter 2002	G+P	Rural	15	**352	(Albinet et al., 2008a)
Danmark, Risø	Winter 1998	P	Semi-rural	4	152	(Feilberg et al., 2001)
Central Europe, Košetice	Winter 2017	G+P	Background	8	15	(Lammel et al., 2020)
Southern Sweden, Råö	Spring 2008	G+P	Background	8	40	(Brorström-Lundén et al., 2010)
Subarctic Finland, Pallas	Spring 2008	G+P	Background	8	19	(Brorström-Lundén et al., 2010)
Arctic, Svalbard, UNIS	Autumn 2018	G+P	Semi-urban	11	37	This study
Arctic, Svalbard, Adventdalen	Autumn 2018	G+P	Rural	11	27	This study
Oxy-PAHs						
Northern China	Annual 2010-2011	G+P	Rural	3	**10552	(Li et al., 2015)
Southern China, Wanqingsha	Autumn 2010	G+P	Rural	5	12940	(Huang et al., 2014b)
France, Marseille	Summer 2004	G+P	Rural	4	1093	(Albinet et al., 2007)
France, The Alps, Chamonix	Winter 2002	P	Rural, altitude	5	790	(Albinet et al., 2008a)
France, The Alps, Maurienne	Winter 2002	G+P	Rural	5	**6875	(Albinet et al., 2008a)
Central Europe, Košetice	Winter 2017	G+P	Rural	5	336	(Lammel et al., 2020)
Eastern England, Weybourne	Winter 2010	G+P	Rural	4	591	(Alam et al., 2014)
Southern Sweden, Råö	Spring 2008	G+P	Background	4	583	(Brorström-Lundén et al., 2010)
Subarctic, Finland, Pallas	Spring 2008	G+P	Background	4	239	(Brorström-Lundén et al., 2010)
Arctic, Svalbard, UNIS	Autumn 2018	G+P	Semi-urban	6	471	This study
Arctic, Svalbard, Adventdalen	Autumn 2018	G+P	Rural	6	233	This study

*within similar detectable compounds

**average of sites within type of site

Table S15. Spearman correlation of selected PAH %PMs with ambient temperature and specific humidity for Adventdalen data (n=6)

	Temperature	Humidity
%PM Fluorene	-0.030	-0.030
%PM Phenanthrene	0.131	0.131
%PM Anthracene	-0.393	-0.393
%PM Fluoranthene	-0.371	-0.371
%PM Pyrene	-0.429	-0.429
%PM Chrysene	**-0.700**	**-0.700**
%PM 1-Nitronaphthale	-0.655	-0.655
%PM 2-Nitronaphthale	-0.698	-0.698
%PM 2-Nitrobiphenyl	-0.455	-0.455
%PM 9-Fluorenone	-0.516	-0.516
%PM 9,10-Anthraquinone	-0.205	-0.205
%PM cPPhen-4	**-0.759**	**-0.759**
%PM 2+3-Nitrofluoranthene	**-0.872**	**-0.872**
%PM 2-NFlu	-0.030	-0.030
%PM 9-NAnt	0.900	0.900

Table S16. Spearman correlation of selected PAH concentrations (G+P) with precipitation for UNIS data (n=6)

	Precipitation
Pyrene	-0.829
Phenanthrene	-0,543
Fluoranthene	-0,543
Chrysene	-0.943
Benzo(b+k)fluoranthene	-0.886
Indeno(1,2,3-cd)pyrene	-0.812
Benzo(g,h,i)perylene	-0.886
Benzo(a)fluoren-11-one	-0.714
Benzo(a)anthracene-7,12-dione	-0.829

Table S17. Spearman correlation of PAH concentrations (G+P) with weather parameters for Adventdalen data (n=6)

	Solar radiation	Temperature	Humidity
Acenaphtylene	**-0.829**	**-1.000**	**-1.000**
Acenaphthene	-0.600	-0.771	-0.771
Fluorene	-0.486	-0.714	-0.714
Phenanthrene	-0.371	-0.657	-0.657
Anthracene	-0.543	-0.714	-0.714
Fluoranthene	**-0.943**	-0.771	-0.771
Pyrene	**-0.886**	**-0.886**	**-0.886**
Chrysene	-0.600	-0.771	-0.771
1-Nitronaphthale	-0.771	**-0.943**	**-0.943**
2-Nitronaphthale	-0.257	-0.429	-0.429
9-Fluorenone	-0.543	**-0.829**	**-0.829**
9,10-Anthraquinone	0.086	-0.314	-0.314
cPPen-4	-0.771	-0.771	-0.771
2-Nitrofluorene	0.200	0.086	0.086
9-Nitroanthracene	0.657	0.714	0.714
Benzo(a)fluoren-11-one	-0.600	-0.771	-0.771
2+3-Nitrofluoranthene	0.657	0.657	0.657

Table S18. %PM obtained in this study compared to literature data

	UNIS[1)]	Adventdalen[1)]	Southern China[2)]	Southeastern France[3)]	The Apls, France[4)]
	Sub-urban, autumn	Rural, autumn	Rural, autumn	Urban, annual	Rural, winter
Acenaphtylene	0 ± 0.0	0 ± 0	0.9	-	-
Acenaphthene	0 ± 0.0	0 ± 0	1.9	5.9	-
Fluorene	1.1 ± 1.0	1.8 ± 3.0	1.3	2.0	-
Phenanthrene	6.5 ± 8.6	3.7 ± 9.0	0.6	3.0	-
Anthracene	0 ± 0.0	3.5 ± 8.5	3.4	4.3	-
Fluoranthene	40.5 ± 19.4	23.2 ± 9.2	11.0	15.7	-
Pyrene	26.8 ± 18.6	15.8 ± 11.0	16.5	20.0	-
Benzo(a)anthracene	68.2 ± 2.4	-	85.3	65.7	-
Chrysene	81.7 ± 10.3	64.1 ± 18.7	85.3	80.7	-
Benzo(b+k)fluoranthene	100 ± 0.0	100 ± 0	98.4	100.0	-
Benzo(a)pyrene	100 ± 0.0	100 ± 0	98.8	100.0	100.0
Indeno(1,2,3-cd)pyrene	100 ± 0.0	100 ± 0	99.6	98.1	-
Dibenzo(a,h)anthracene	-	-	100.0	100.0	-
Benzo(g,h,i)perylene	100 ± 0.0	100 ± 0	99.6	97.8	-
1-Nitronaphthalene	0.1 ± 0.2	1.5 ± 3.6	1.7	2.1	11.3
2-Nitronaphthalene	3.1 ± 5.6	5.4 ± 8.0	0.7	2.3	8.5
2-Nitrobiphenyl	10.1 ± 8.3	5.9 ± 10.0	14.5	0	-
9-Fluorenone	41.7 ± 22.3	25.5 ± 13.4	3.8	2.2	38.8
4-Nitrobiphenyl	0 ± 0.0	-	3.8	-	-
1,5-Dinitronaphthalene	80.0 ± 44.7	53.9 ± 53.6	39.3	100.0	-
9,10-Anthraquinone	37.5 ± 22.4	43.9 ± 1.4	43.0	55.8	97.8
5-Nitroacenaphthene	-	-	95.0	53.3	-
cPPhen-4	65.5 ± 10.6	38.1 ± 20.2	20.4	-	-
2-Nitrofluorene	15.1 ± 7.5	4.2 ± 9.5	-	0.0	87.5
9-Nitroanthracene	-	57.8 ± 29.7	95.0	64.7	95.8
9-Nitrophenanthrene	-	25 ± 50	-	66.7	88.3
Benzo(a)fluoren-11-one	100 ± 0.0	100 ± 0	-	95.5	99.8
Benzanthrone	96.7 ± 4.8	100 ± 0	98.2	100.0	100.0
2+3-Nitrofluoranthene	94.5 ± 13.5	79.8 ± 16.5	97.0	98.6	99.0
Benzo(a)anthracene-7,12-dione	100 ± 0.0	100 ± 0	99.3	99.4	100.0

[1)]This study; [2)] (Huang et al., 2014a); [3)] (Tomaz et al., 2016); [4)] (Albinet et al., 2008b)

Table S19. Combustion engine vehicles in Longyearbyen as of 2018

	Diesel engine	Gasoline engine	Total
Passenger cars	522	553	1114
Vans	276	17	293
Lorry	52	8	60
Buses	26	-	26
Tractors	33	32	65
Recreational Boats	n.a.	n.a.	718

290

Data acquired from Statistics Norway (www.ssb.no), last access: 20 June 2020
n.a. this information is not available

Table S20. Eigenanalysis of the correlation matrix and Eigenvectors for Adventdalen data

Variable	PC1	PC2
Eigenvalue	8,7122	3,8497
Proportion	**0,512**	**0,226**
Cumulative	0,512	0,739
Flu/(Flu+Pyr)	-0,002	**-0,427**
IPyr/(IPyr+BPer)	**0,238**	0,225
Flu	0,207	**-0,366**
Phe	**0,176**	**-0,388**
Flt	**0,243**	0,294
Pyr	**0,300**	0,225
9-Flu	0,170	**-0,287**
9,10-AntQ	0,153	-0,090
cPPhe-4	**0,319**	0,096
BaFlu-11	**0,285**	0,194
BaAnt-7,12	**0,240**	0,047
1-NNap	0,253	**-0,308**
9-NAnt	**-0,225**	0,054
2+3-NFlt	**-0,245**	-0,252
Temperature	**-0,318**	0,068
Humidity	**-0,287**	0,187
Solar Radiation	**-0,264**	-0,073

Table S21. Spearman correlation of PAH concentrations (G+P; n=6) with diagnostic ratios for Adventdalen data

	IPyr/(IPyr+BPer) traffic	Flu/(Flu+Pyr) coal burning
Flu	0,270	**0,771**
Phe	0,101	**0,771**
Ant	**0,845**	0,143
Flt	0,541	-0,257
Pyr	0,439	0,257
Chry	**0,778**	-0,029
1-NNap	0,439	0,429
9-Flu	-0,034	0,314
9,10-AntQ	-0,101	0,257
cPPhe-4	**0,778**	-0,314
9-NAnt	-0,135	-0,371
9-NPhe	**0,789**	-0,232
BaFlu-11	**0,778**	-0,029
2+3-NFlt	-0,778	0,086
BaAnt-7,12	**0,845**	0,143

Table S22. Extractions from certificate of quality: unleaded gasoline, RON95, Norway, summer

Property	Units	Spec	Results
Appearance	-	Clear % Bright	Clear & Bright
Density at 15 deg. C	kg/m3	720-775	723.0
Reid Vapour Pressure	kPa	≤ 67.0	66.9
Colour	-	Undyed	Undyed
Odour	-		Merchantable
Total Sulphur	mg/kg	≤ 10.0	3.9
Copper Strip Corrosion 3h at 50 deg. C	-	No.1	No.1
Existent Gum	mg/100ml	≤ 5	≤ 5
Oxidation Stability	min	≥ 360	≥ 360
MTBE	%-vol	≤ 0.5	<0.1
Oxygen content	%-wt	≤ 0.5	<0.1
Other Oxygenates		Not allowed	Not added
Lead	mg_Pb/l	≤ 5	≤ 3
Manganese	mg/l	≤ 2	≤ 2
Evaporated at 70 deg. C	%-vol	22.0-48.0	37.4
Evaporated at 100 deg. C	%-vol	46.0-71.0	60.9
Evaporated at 150 deg. C	%-vol	≥ 75.0	90.8
Final Boiling Point	deg. C	≤ 210.0	195.0
Residue	%-vol	≤ 2.0	1.0
Olefins	%-vol	≤ 18.0	17.5
Aromatics	%-vol	≤ 35.0	19.7
Benzene	%-vol	≤ 1.00	0.84
Motor Octane Number	-	≥ 85.0	85.0
Research Octane Number	-	≥ 95.0	95.0
Silver strip corrosion (3h at 50 deg. C)	-	≤ 1	0

Table S23. Extractions from certificate of quality: B-base automotive diesel, CFPP-12, Norway

Property	Units	Spec	Results
Appearance at 20 deg. C	-	Clear & Bright	Clear & Bright
Water	ppm-wt	≤ 100	≤ 100
Density at 15 deg. C	kg/m3	820.0-842.0	840.8
Recovered at 250 deg. C	%-vol	≤ 64	40
Recovered at 350 deg. C	%-vol	≥ 85	98
95% Recovered	deg. C	≤ 360	332
Flash Point	deg. C	≥ 58	62
Total Sulphur	mg/kg	≤ 10.0	9.8
Copper Strip Corrosion 3h at 50 deg. C	-	No. 1	No. 1
Oxidation Stability	g/m3	≤ 25	≤ 25
Viscosity at 40 deg. C	mm2/s	2.00-4.00	2.57
Lubricity at 60 deg. C	um	≤ 460	≤ 460
Cloud Point	deg. C	≤ -1	-17
Cold Filter Plugging Point	deg. C	≤ -12	-17
Carbon Residue on 10 % Residue	%-wt	≤ 0.30	≤ 0.30
Ash	%-wt	≤ 0.01	≤ 0.01
Manganese	mg/l	≤ 2.0	≤ 2.0
Particulate Matter	mg/kg	≤ 24	≤ 24
Fatty acid methyl ester	%-vol	≤ 0.2	≤ 0.2
PAH	%-wt	≤ 8.0	3.4
Cetane Index, four variable	-	≥ 46.0	48.8
Cetane Number	-	≥ 51.0	51.6
Aromatics, %-wt	%-wt	Report	26.4
Conductivity	pS/m	>=50	218
at temperature	deg. C	Report	22
Stadis 425	mg/l	Report	2.0

Table S24. Ratios of nitro- and oxy-PAH to corresponding parent PAH at three locations

	Power plant (n=6)			UNIS (n=6)			Adventdalen (n=6)		
	Mean	STD	Median	Mean	STD	Median	Mean	STD	Median
9,10-AntQ/Ant	12.16	6.53	10.47	9.44	3.80	7.63	4.02	2.40	4.57
9-NAnt/Ant	0.055	0.020	0.056	0.039	0.026	0.042	0.189	0.171	0.109
9-FluQ/Flu	1.67	0.29	1.72	1.65	0.95	1.30	2.35	0.79	2.15
BaFlu-11/Chry	0.65	0.34	0.58	0.87	0.26	0.82	0.67	0.15	0.63
cPPhen-4/Pyr	0.31	0.10	0.30	0.64	0.30	0.56	0.48	0.06	0.48
9-FluQ/Phe	0.47	0.13	0.42	0.67	0.38	0.51	0.55	0.09	0.56
2+3-NFlt/Flt	0.029	0.023	0.017	0.335	0.043	0.324	0.603	0.326	0.585

Table S25. Spearman correlation of nitro- and oxy-PAH to corresponding parent PAH ratios with weather parameters in Adventdalen (n=6)

	Solar radiation	Temperature	Humidity	Pressure
9-Flu/Flu	0.029	0.029	0.029	-0.029
9,10-AntQ/Ant	0.486	-0.029	-0.029	0.429
9-FluQ/Phe	-0.429	-0.486	-0.486	-0.257
9-NAnt/Ant	0.600	**0.829**	**0.829**	0.543
2+3-NFlt/Flt	**0.886**	**0.714**	**0.829**	**0.943**
cPPhen-4/Pyr	0.257	0.257	0.257	-0.029

Table S26. Spearman correlation of concentrations (G+P) of PAHs, nitro- and oxy-PAHs with each other for Adventdalen data (n=6)

	Acy	Ace	Flu	Phe	Ant	Flt	Pyr	Chry	1-Nnap	2-Nnap	9-Flu	9,10-AntQ	cPPhen-4	2-Nflu	9-Nant	9-NPhe	BaFlu-11	2+3-NFlt	BaAnt-7,12
Acy																			
Ace	0.771																		
Flu	0.714	0.600																	
Phe	0.657	0.314	0.829																
Ant	0.714	0.943	0.714	0.486															
Flt	0.771	0.714	0.314	0.143	0.600														
Pyr	0.886	0.600	0.657	0.714	0.657	0.771													
Chry	0.771	1.000	0.600	0.314	0.943	0.714	0.600												
1-Nnap	0.943	0.714	0.829	0.829	0.771	0.657	0.943	0.714											
2-Nnap	0.429	0.029	0.714	0.943	0.257	-0.029	0.600	0.029	0.657										
9-Flu	0.829	0.371	0.486	0.714	0.314	0.429	0.714	0.371	0.771	0.543									
9,10-AntQ	0.314	0.429	0.371	0.086	0.257	-0.029	-0.143	0.429	0.143	-0.143	0.257								
cPPhen-4	0.771	0.829	0.314	0.257	0.771	0.886	0.771	0.829	0.714	0.029	0.486	-0.029							
2-Nflu	-0.086	-0.143	0.600	0.429	0.029	-0.429	-0.086	-0.143	0.086	0.543	-0.143	0.257	-0.543						
9-Nant	-0.714	-0.657	-0.714	-0.314	-0.543	-0.600	-0.486	-0.657	-0.600	-0.143	-0.371	-0.600	-0.371	-0.314					
9-NPhe	0.812	0.899	0.406	0.319	0.841	0.841	0.754	0.899	0.754	0.058	0.522	0.116	0.986	-0.464	-0.435				
BaFlu-11	0.771	1.000	0.600	0.314	0.943	0.714	0.600	1.000	0.714	0.029	0.371	0.429	0.829	-0.143	-0.657	0.899			
2+3-NFlt	-0.657	-0.943	-0.543	-0.143	-0.886	-0.771	-0.543	-0.943	-0.600	0.086	-0.143	-0.314	-0.771	0.086	0.714	-0.812	-0.943		
BaAnt-7,12	0.714	0.943	0.714	0.486	1.000	0.600	0.657	0.943	0.771	0.257	0.314	0.257	0.771	0.029	-0.543	0.841	0.943	-0.886	

310

Table S27. Eigenanalysis of the correlation matrix and Eigenvectors for UNIS data

Variable	PC1	PC2
Eigenvalue	8,9948	3,5126
Proportion	**0,529**	**0,207**
Cumulative	0,529	0,736
BbkFlt/BPer	**0,235**	-0,066
Flu/(Flu+Pyr)	-0,195	**-0,326**
Flt/(Flt+ Pyr)	-0,062	**0,458**
Phe	-0,117	**-0,426**
Flt	**0,294**	0,162
Pyr	**0,308**	-0,110
Chry	**0,289**	-0,217
BaPyr	**0,323**	0,071
BPer	**0,266**	-0,284
1-NNap	**0,193**	-0,057
2-NNap	**0,303**	0,119
9-Flu	-0,093	**0,274**
9,10-AntQ	-0,182	**-0,374**
cPPeh-4	0,076	**0,203**
BaFlu-11	**0,320**	-0,056
BZT	**0,282**	0,100
BaAnt-7,12	**0,302**	-0,203

Table S28. Spearman correlation of PAH concentrations (G+P; n=6) with diagnostic ratios for UNIS data

	IPyr/(IPyr+BPer) traffic	BbkFlt/BPer diesel/gasoline	Flu/(Flu+Pyr) coal combustion	Flt/(Flt+Pyr) marine fuel
Flu	-0,429	0,143	**0,714**	-0,714
Phe	0,086	0,200	**0,543**	-0,200
Flt	0,886	**0,771**	-0,829	0,143
Pyr	0,771	**0,886**	-0,714	-0,143
Chry	0,543	**0,886**	-0,371	-0,486
BbkFlt	0,600	**0,943**	-0,200	-0,314
BaPyr	0,759	**0,880**	-0,698	-0,030
IPyr	0,754	**0,986**	-0,464	-0,232
BPer	0,600	**0,943**	-0,200	-0,314
1-NNap	**0,543**	0,429	-0,600	-0,086
2-NNap	**0,771**	0,657	-0,943	0,086
9-Flu	0,371	0,257	0,029	**0,657**
9,10-AntQ	-0,829	-0,600	**0,657**	-0,486
cPPeh-4	0,086	0,314	0,314	0,200
BaFlu-11	**0,771**	**0,886**	-0,714	-0,143
BZT	**0,754**	0,638	-0,696	0,087
BaAnt-7,12	**0,714**	**0,943**	-0,543	-0,314

315

Figure S1. Wind rose diagrams for UNIS (samples U1-U7) and Adventdalen (samples A1-A7) sampling stations

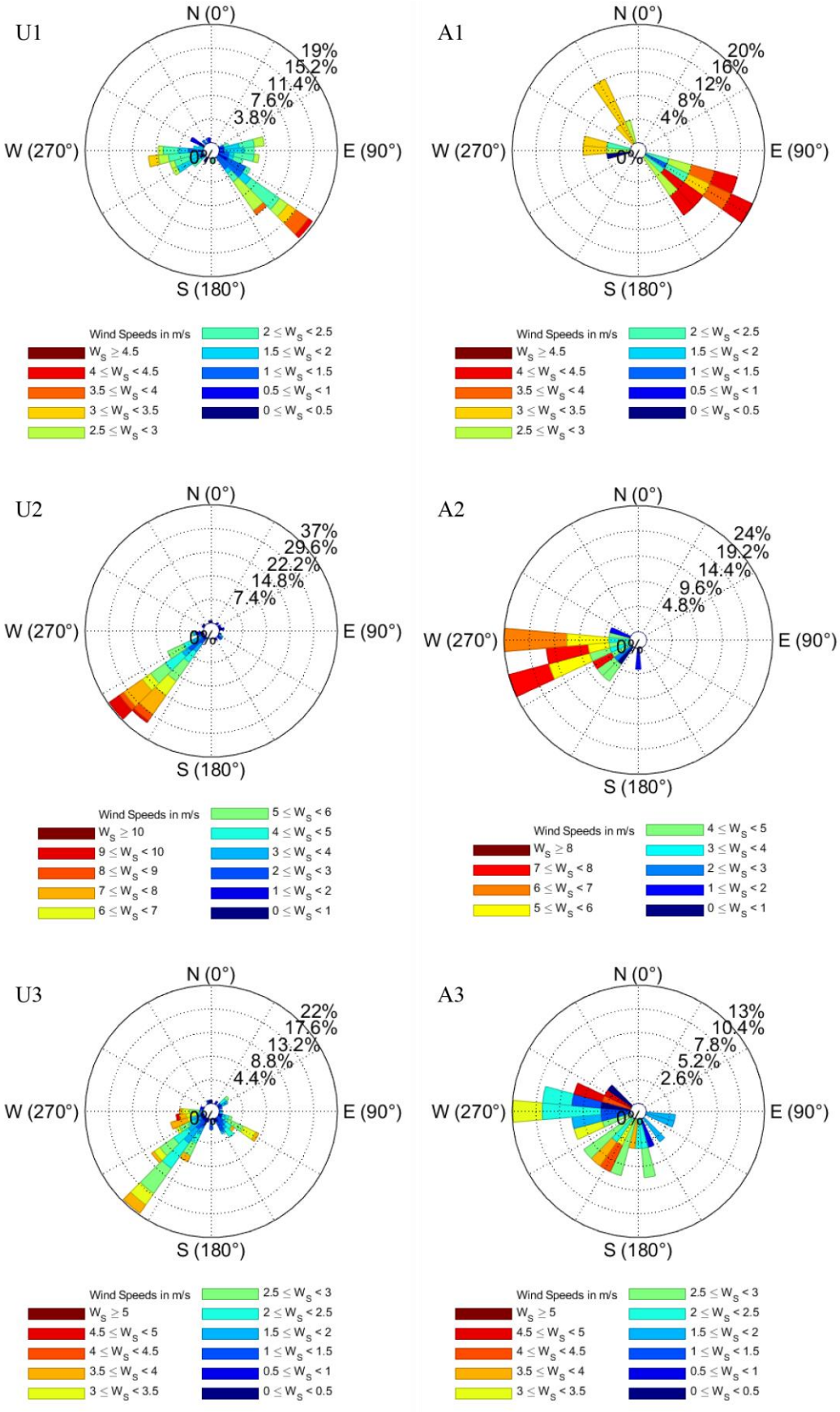

Figure S1 continued

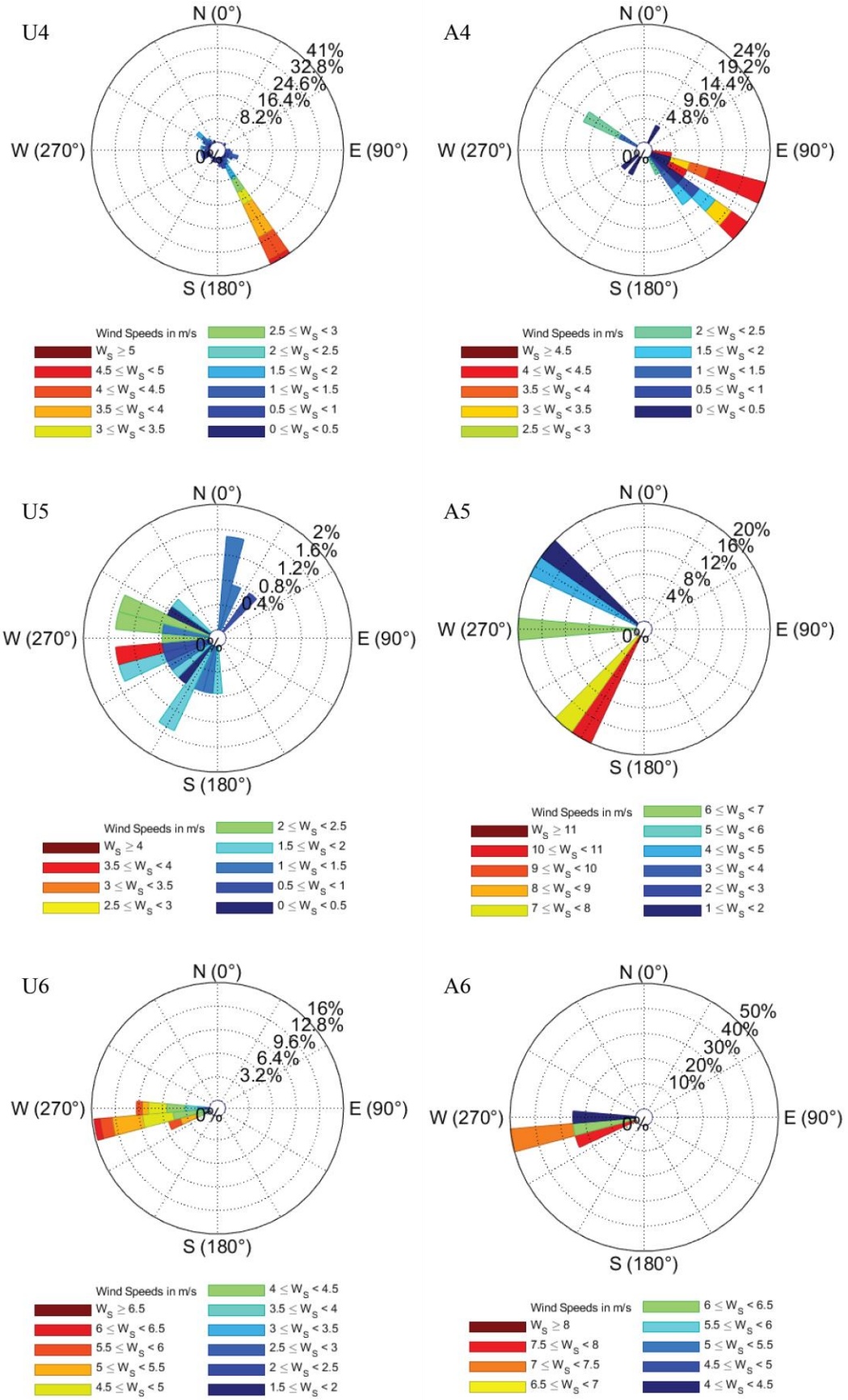

320

Figure S1 continued

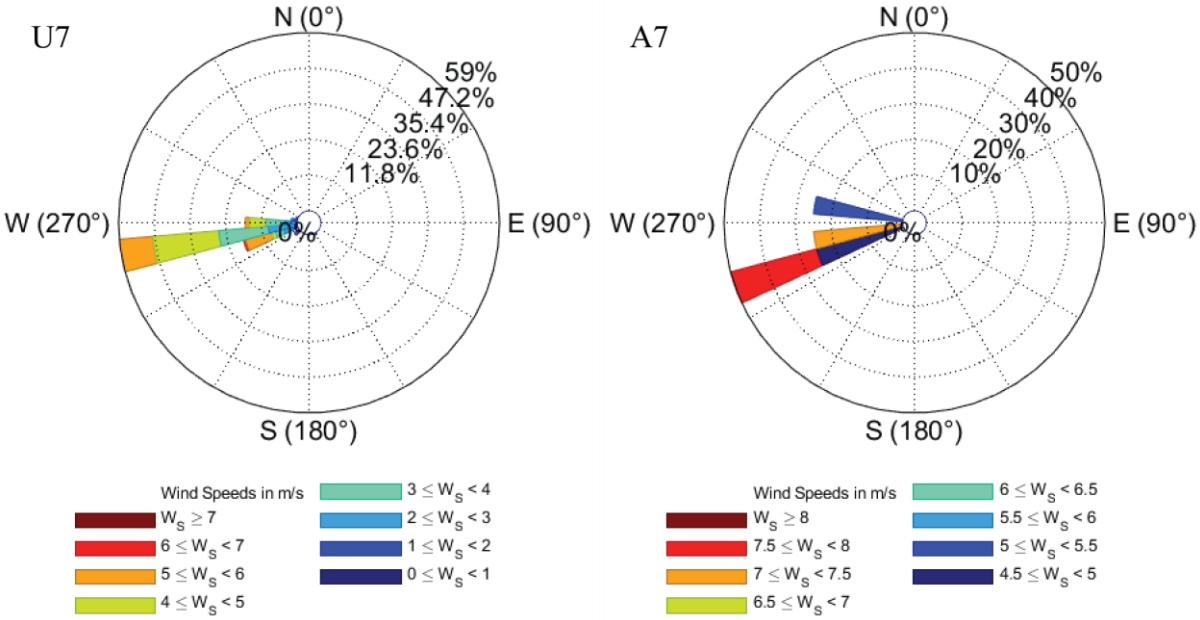

Figure S2. UNIS and Adventdalen chemical profiles of (a) PAHs, (b) oxy-PAHs, and (c) nitro-PAHs

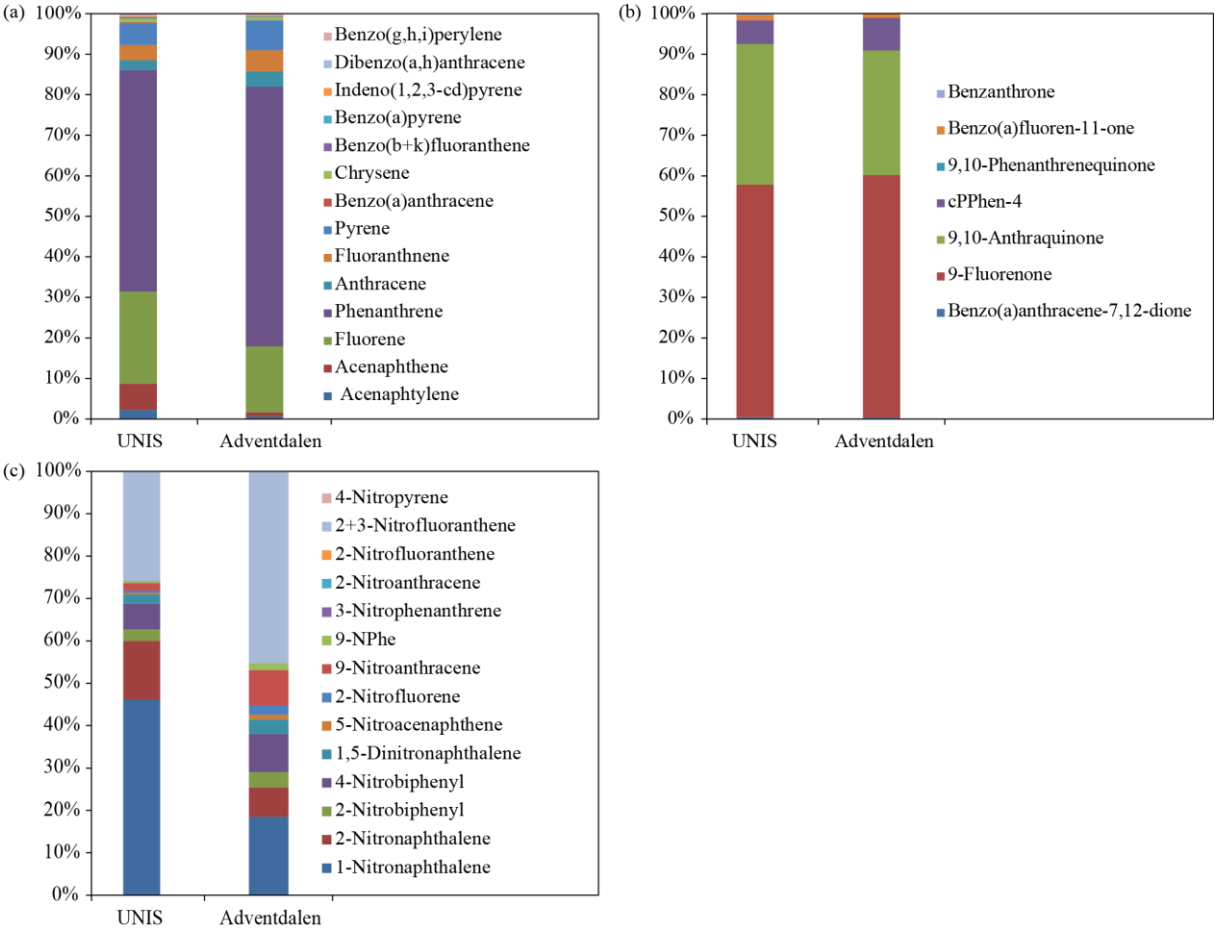

Figure S3. The 15 PAH profiles for different stations in Svalbard (UNIS, Adventdalen, Zeppelin) and the mainland Norway (Birkenes) measured in *autumn 2018

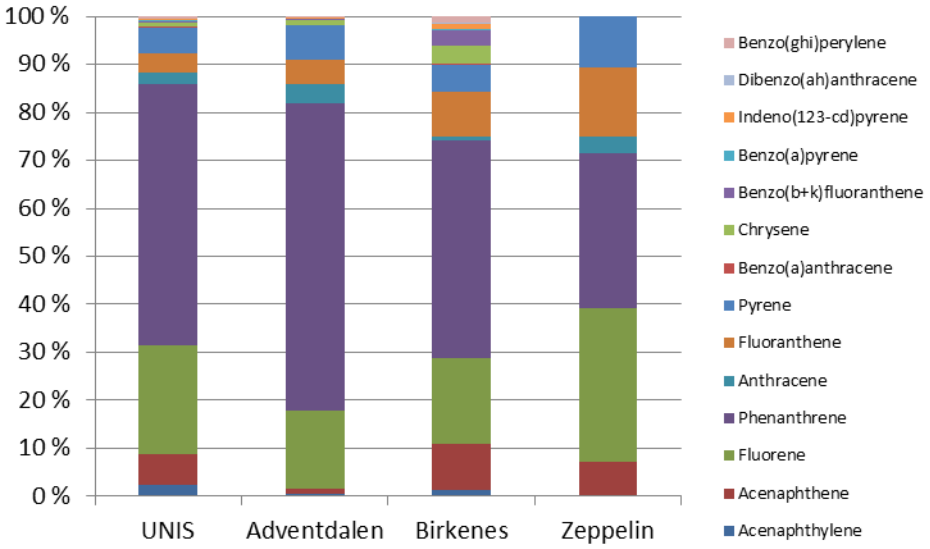

* Based on Table S13 data

330

Figure S4. 5-day back trajectories of Longyearbyen*

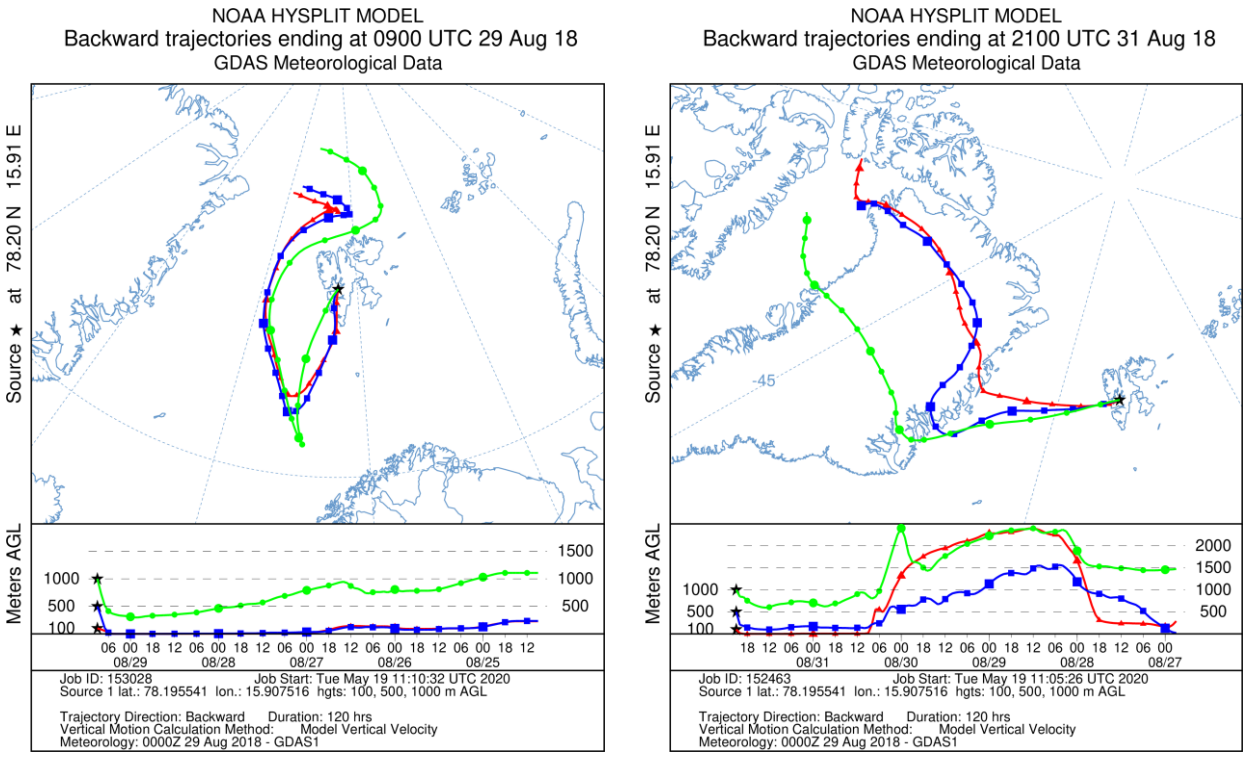

Figure S4 continued

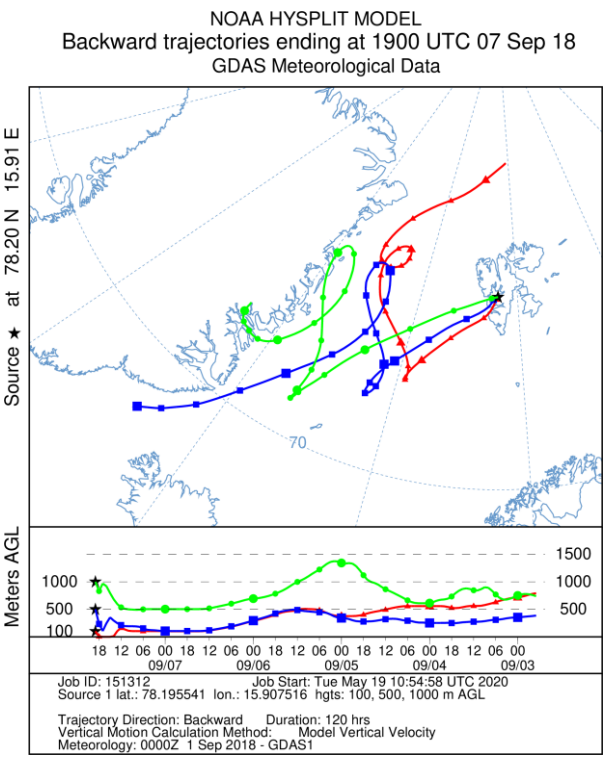

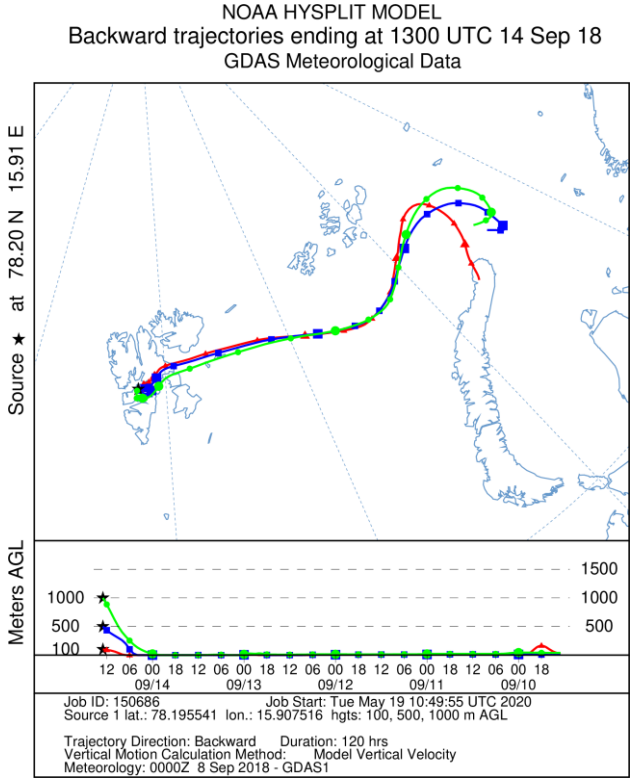

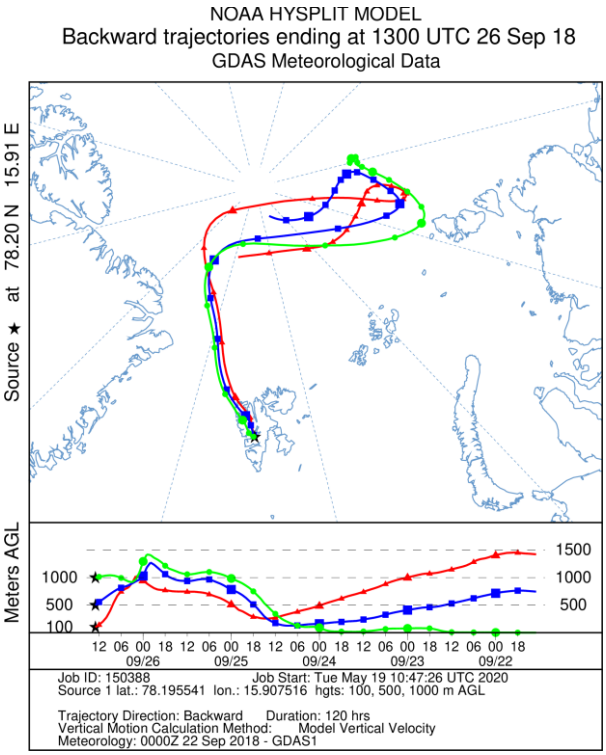

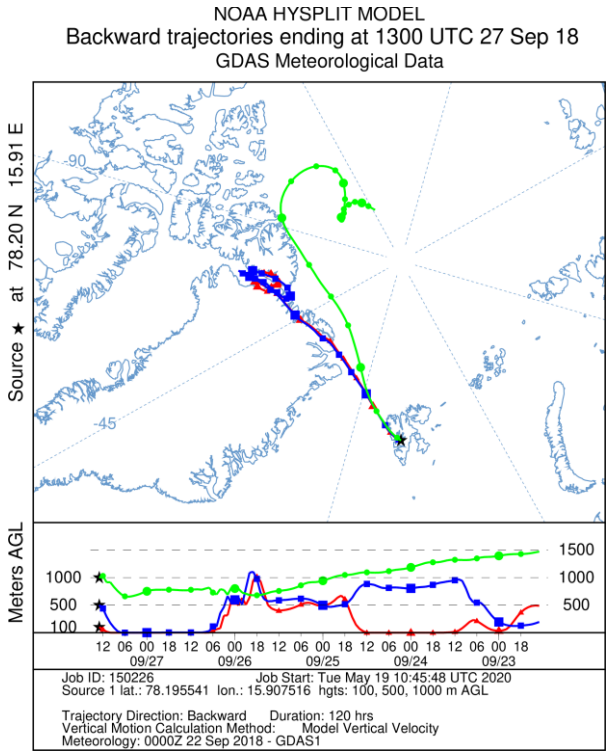

Figure S4 continued

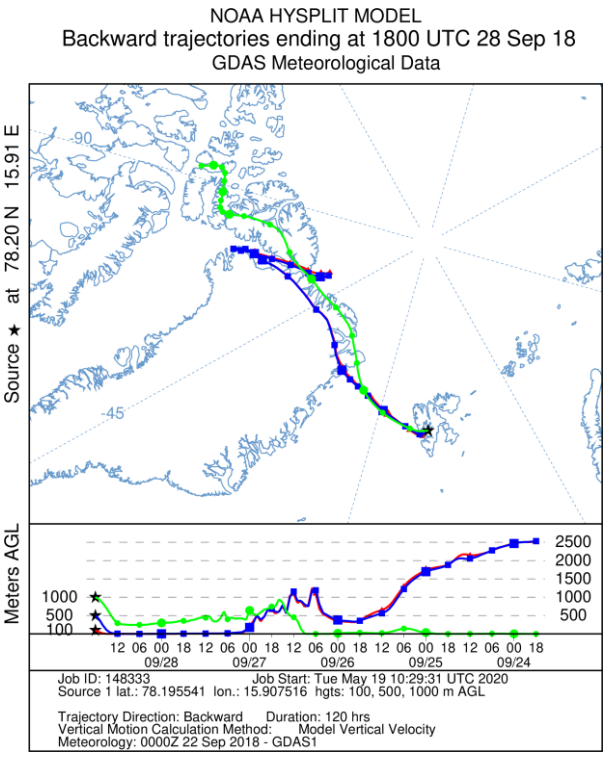

*calculated using the US NOAA Hybrid Single Particle Lagrangian Integrated Trajectory (HYSPLIT) model

Figure S5. Port Longyearbyen statistics 2018

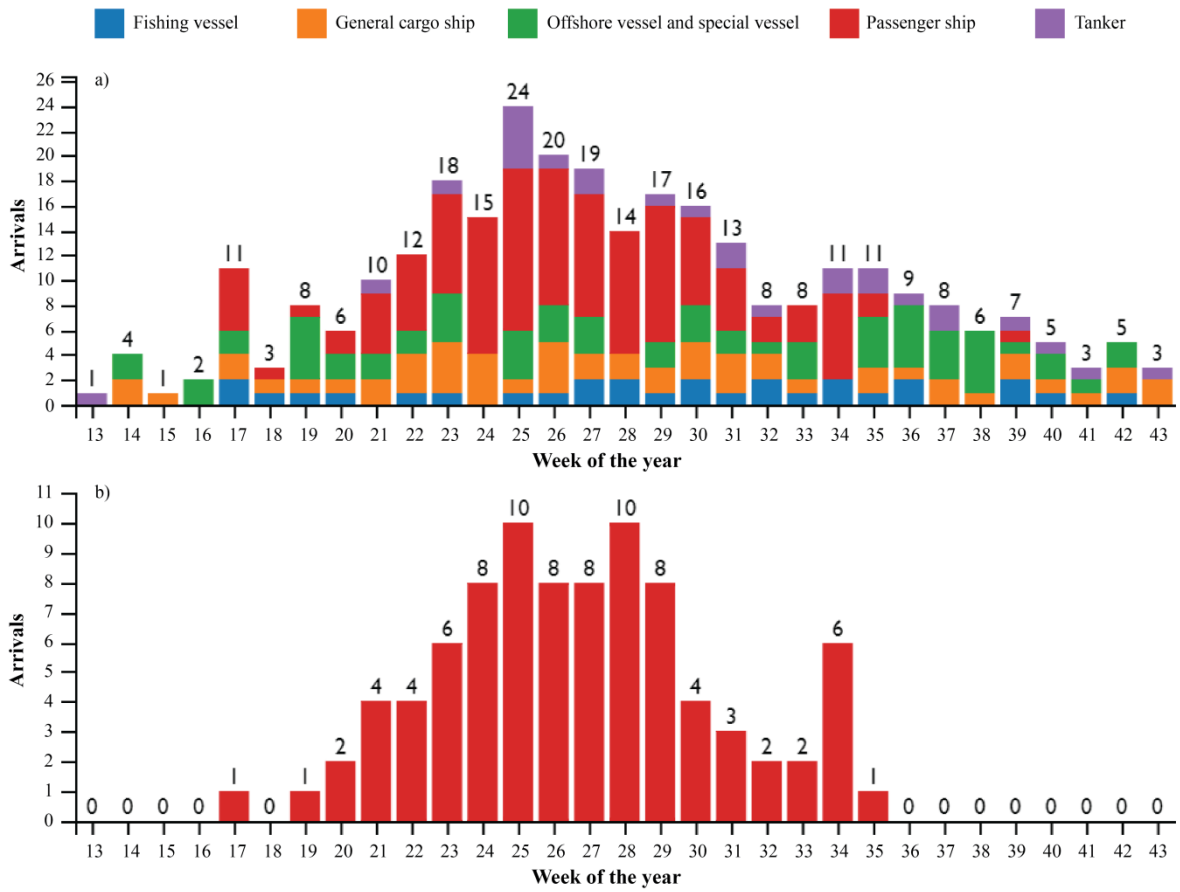

*data acquired from https://kystdatahuset.no/, last access: 30 May 2020

**this study sampling was performed during week 34-38 period

References

Alam, M. S., Delgado-Saborit, J. M., Stark, C., and Harrison, R. M.: Investigating PAH relative reactivity using congener profiles, quinone measurements and back trajectories, Atmos. Chem. Phys., 14, 2467-2477, https://doi.org/10.5194/acp-14-2467-2014, 2014.

Albinet, A., Leoz-Garziandia, E., Budzinski, H., and ViIlenave, E.: Simultaneous analysis of oxygenated and nitrated polycyclic aromatic hydrocarbons on standard reference material 1649a (urban dust) and on natural ambient air samples by gas chromatography–mass spectrometry with negative ion chemical ionisation, J. Chromatogr. A, 1121, 106-113, https://doi.org/10.1016/j.chroma.2006.04.043, 2006.

Albinet, A., Leoz-Garziandia, E., Budzinski, H., and ViIlenave, E.: Polycyclic aromatic hydrocarbons (PAHs), nitrated PAHs and oxygenated PAHs in ambient air of the Marseilles area (South of France): Concentrations and sources, Science of the Total Environment, 384, 280-292, 10.1016/j.scitotenv.2007.04.028, 2007.

Albinet, A., Leoz-Garziandia, E., Budzinski, H., Villenave, E., and Jaffrezo, J. L.: Nitrated and oxygenated derivatives of polycyclic aromatic hydrocarbons in the ambient air of two French alpine valleys - Part 1: Concentrations, sources and gas/particle partitioning, Atmos. Environ., 42, 43-54, https://doi.org/10.1016/j.atmosenv.2007.10.009, 2008a.

Albinet, A., Leoz-Garziandia, E., Budzinski, H., Villenave, E., and Jaffrezo, J. L.: Nitrated and oxygenated derivatives of polycyclic aromatic hydrocarbons in the ambient air of two French alpine valleys. Part 1: Concentrations, sources and gas/particle partitioning, Atmos. Environ., 42, 43-54, http://doi.org/10.1016/j.atmosenv.2007.10.009, 2008b.

Albinet, A., Tomaz, S., and Lestremau, F.: A really quick easy cheap effective rugged and safe (QuEChERS) extraction procedure for the analysis of particle-bound PAHs in ambient air and emission samples, Sci. Total Environ., 450-451, 31-38, https://doi.org/10.1016/j.scitotenv.2013.01.068, 2013.

Albinet, A., Nalin, F., Tomaz, S., Beaumont, J., and Lestremau, F.: A simple QuEChERS-like extraction approach for molecular chemical characterization of organic aerosols: application to nitrated and oxygenated PAH derivatives (NPAH and OPAH) quantified by GC–NICIMS, Anal. Bioanal.Chem., 406, 3131-3148, https://doi.org/10.1007/s00216-014-7760-5, 2014.

Brorström-Lundén, E., Remberger, M., Kaj, L., Hansson, K., Palm Cousins, A., and Andersson, H.: Results from the Swedish national screening programme 2008, IVL Swedish Environmental Research Institute, Göteborg, Sweden, 69, 2010.

Burns, D. T., Danzer, K., and Townshend, A.: Use of the term" recovery" and" apparent recovery" in analytical procedures (IUPAC Recommendations 2002), Pure Appl. Chem., 74, 2201-2205, https://doi.org/10.1351/pac200274112201., 2002.

Feilberg, A., Poulsen, M. W. B., Nielsen, T., and Skov, H.: Occurrence and sources of particulate nitro-polycyclic aromatic hydrocarbons in ambient air in Denmark, Atmos. Environ., 35, 353-366, https://doi.org/10.1016/s1352-2310(00)00142-4, 2001.

Han, M., Kong, J., Yuan, J., He, H., Hu, J., Yang, S., Li, S., Zhang, L., and Sun, C.: Method development for simultaneous analyses of polycyclic aromatic hydrocarbons and their nitro-, oxy-, hydroxy- derivatives in sediments, Talanta, 205, 120128, https://doi.org/10.1016/j.talanta.2019.120128, 2019.

Hsu, W. T., Liu, M. C., Hung, P. C., Chang, S. H., and Chang, M. B.: PAH emissions from coal combustion and waste incineration, J. Hazard. Mater., 318, 32-40, http://doi.org/10.1016/j.jhazmat.2016.06.038, 2016.

Huang, B., Liu, M., Bi, X., Chaemfa, C., Ren, Z., Wang, X., Sheng, G., and Fu, J.: Phase distribution, sources and risk assessment of PAHs, NPAHs and OPAHs in a rural site of Pearl River Delta region, China, Atmos. Pollut. Res., 5, 210-218, https://doi.org/10.5094/APR.2014.026, 2014a.

Huang, B., Liu, M., Bi, X. H., Chaemfa, C., Ren, Z. F., Wang, X. M., Sheng, G. Y., and Fu, J. M.: Phase distribution, sources and risk assessment of PAHs, NPAHs and OPAHs in a rural site of Pearl River Delta region, China, Atmospheric Pollution Research, 5, 210-218, https://doi.org/10.5094/apr.2014.026, 2014b.

Kanan, R., Andersson, J. T., Receveur, J., Guyomarch, J., Le Floch, S., and Budzinski, H.: Quantification of polycyclic aromatic compounds (PACs), and alkylated derivatives by gas chromatography-tandem mass spectrometry (GC/MS/MS) to qualify a reference oil, in: Proceedings of the Thirty-fifth AMOP technical seminar on environmental contamination and response, Ottawa, Canada, 2012, 616-927, 2012.

Konieczka, P., and Namieśnik, J.: Limit of detection and limit of quantification, in: Quality assurance and quality control in the analytical chemical laboratory, CRC Press, Taylor & Francis Group, Boca Raton, Florida, USA, 143-160, 2009.

Lammel, G., Kitanovski, Z., Kukucka, P., Novak, J., Arangio, A. M., Codling, G. P., Filippi, A., Hovorka, J., Kuta, J., Leoni, C., Pribylova, P., Prokes, R., Sanka, O., Shahpoury, P., Tong, H. J., and Wietzoreck, M.: Oxygenated and nitrated polycyclic aromatic hydrocarbons in ambient air-levels, phase partitioning, mass size distributions, and inhalation bioaccessibility, Environ. Sci. Technol., 54, 2615-2625, https://doi.org/10.1021/acs.est.9b06820, 2020.

Launiainen, J., and Vihma, T.: Derivation of turbulent surface fluxes — An iterative flux-profile method allowing arbitrary observing heights, Environmental Software, 5, 113-124, https://doi.org/10.1016/0266-9838(90)90021-W, 1990.

Li, J., Li, X., Li, M., Lu, S., Yan, J., Xie, W., liu, C., and Qi, Z.: Influence of air pollution control devices on the polycyclic aromatic hydrocarbon distribution in flue gas from an ultralow-emission coal-fired power plant, Energy & Fuels, 30, 9572-9579, http://doi.org/10.1021/acs.energyfuels.6b01381, 2016.

Li, W., Wang, C., Shen, H. Z., Su, S., Shen, G. F., Huang, Y., Zhang, Y. Y., Chen, Y. C., Chen, H., Lin, N., Zhuo, S. J., Zhong, Q. R., Wang, X. L., Liu, J. F., Li, B. G., Liu, W. X., and Tao, S.: Concentrations and origins of nitro-polycyclic aromatic hydrocarbons and oxy-polycyclic aromatic hydrocarbons in ambient air in urban and rural areas in northern China, Environ. Pollut., 197, 156-164, https://doi.org/10.1016/j.envpol.2014.12.019, 2015.

Meij, R., and Te Winkel, H.: The emissions of heavy metals and persistent organic pollutants from modern coal-fired power stations, Atmos. Environ., 41, 9262-9272, https://doi.org/10.1016/j.atmosenv.2007.04.042, 2007.

Observation data of atmospheric PAHs at Zeppelin and Birkenes stations in 2018: http://ebas.nilu.no, access: 25 June 2020, 2018.

Rigamonti, L., Grosso, M., and Biganzoli, L.: Environmental assessment of refuse-derived fuel co-combustion in a coal-fired power plant, J. Ind. Ecol., 16, 748-760, http://doi.org/10.1111/j.1530-9290.2011.00428.x, 2012.

Şengül, Ü.: Comparing determination methods of detection and quantification limits for aflatoxin analysis in hazelnut, J. Food Drug Anal., 24, 56-62, https://doi.org/10.1016/j.jfda.2015.04.009, 2016.

Shrivastava, A., and Gupta, V. B.: Methods for the determination of limit of detection and limit of quantitation of the analytical methods, Chronicles of young scientists, 2, 21, https://doi.org/10.4103/2229-5186.79345, 2011.

Tomaz, S., Shahpoury, P., Jaffrezo, J.-L., Lammel, G., Perraudin, E., Villenave, E., and Albinet, A.: One-year study of polycyclic aromatic compounds at an urban site in Grenoble (France): Seasonal variations, gas/particle partitioning and cancer risk estimation, Sci. Total Environ., 565, 1071-1083, http://doi.org/10.1016/j.scitotenv.2016.05.137, 2016.

Wang, R., Liu, G., and Zhang, J.: Variations of emission characterization of PAHs emitted from different utility boilers of coal-fired power plants and risk assessment related to atmospheric PAHs, Sci. Total Environ., 538, 180-190, http://doi.org/10.1016/j.scitotenv.2015.08.043, 2015.

Yu, Y., Katsoyiannis, A., Bohlin-Nizzetto, P., Brorstrom-Lunden, E., Ma, J. M., Zhao, Y., Wu, Z. Y., Tych, W., Mindham, D., Sverko, E., Barresi, E., Dryfhout-Clark, H., Fellin, P., and Hung, H.: Polycyclic Aromatic Hydrocarbons Not Declining in Arctic Air Despite Global Emission Reduction, Environ. Sci. Technol., 53, 2375-2382, 10.1021/acs.est.8b05353, 2019.